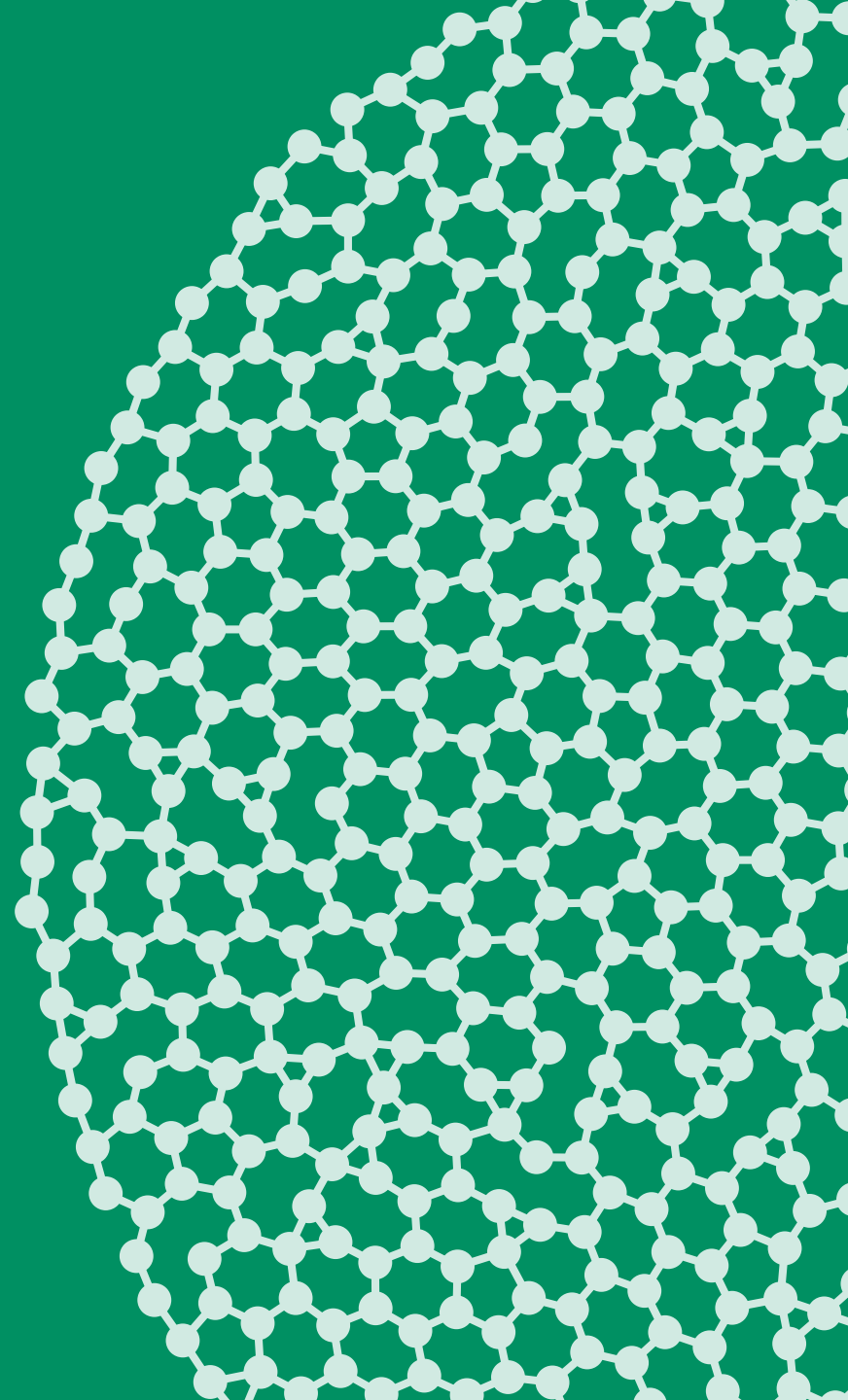




Applications of neutral atom QPUs

April 22, 2024

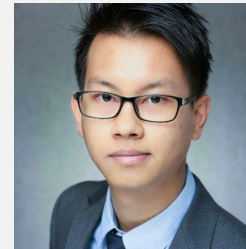


Quantum simulation team @PASQAL

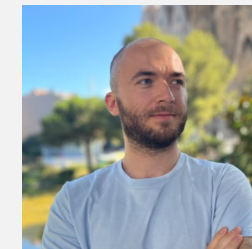
- Quantum simulation schemes tailored for PASQAL's QPU
 - E.g. Amorphous materials
 - Other systems of interest in material science
- Numerical benchmarks
 - Tensor networks
 - Quantum Monte Carlo
 - Semi-analytical methods
 - ...



Alexandre Dauphin (Team Leader)



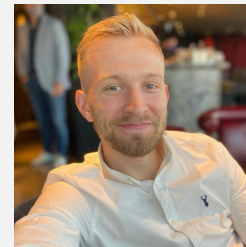
Augustine Kshetrimayum



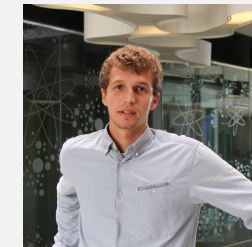
Kemal Bidzhiev



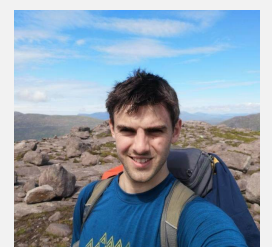
Tiago Mendes-Santos



Joseph Vovrosh



Sergi Julià-Farré



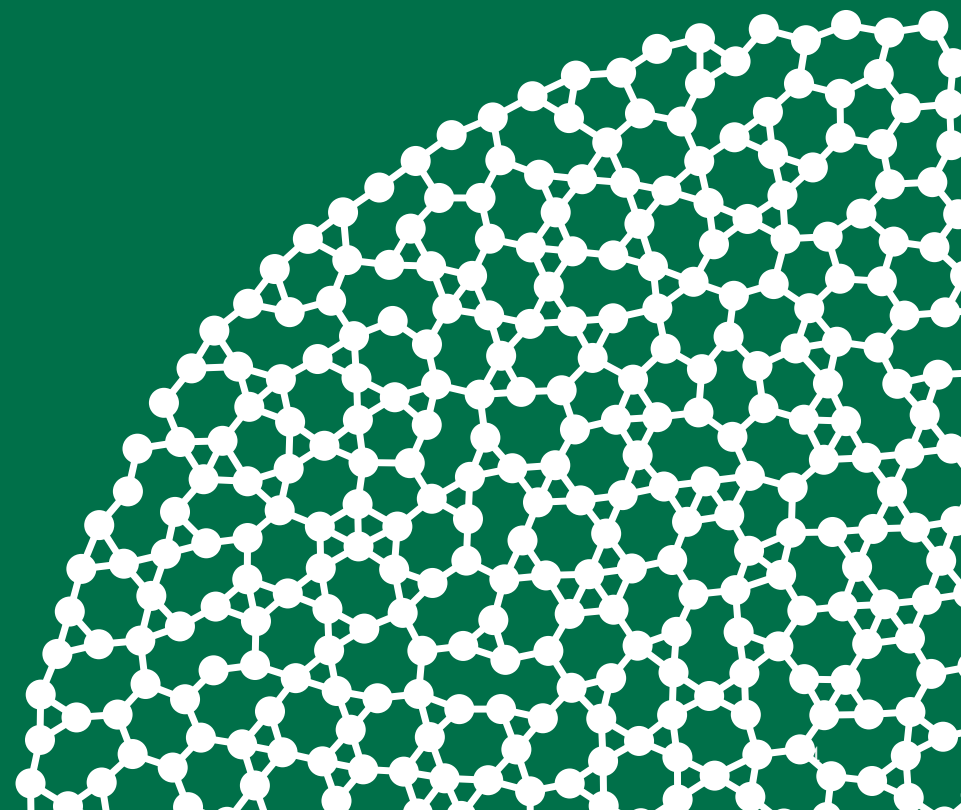
Fergus Hayes

Outline

1. (Brief) review of the neutral atom QPU
2. Optimization: Maximum independent set
3. Quantum Materials: Amorphous quantum magnets
4. Machine learning: Quantum evolution Kernel

1

(Brief) review of the neutral atom QPU



Making Qubits out of atoms

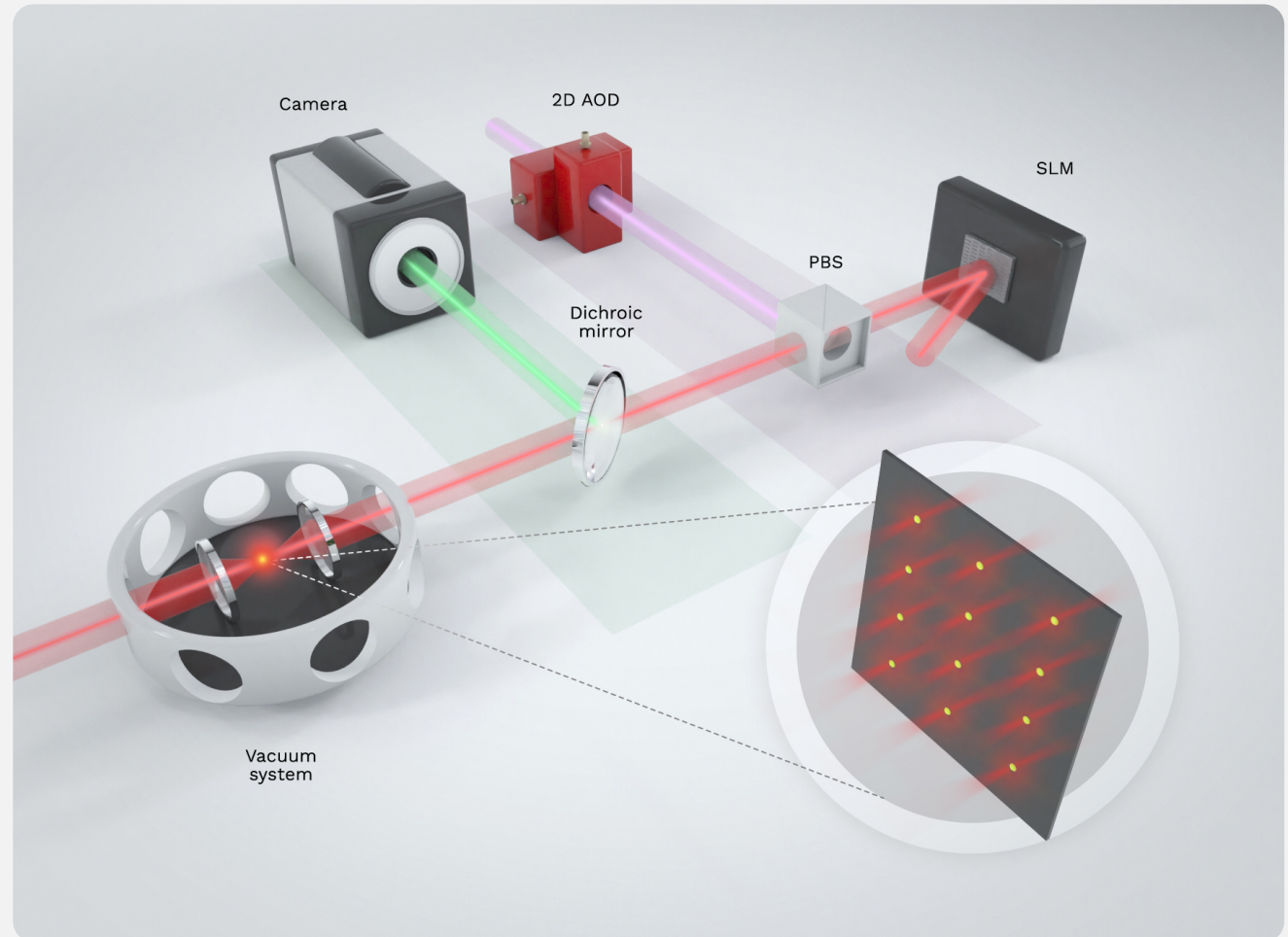
How do we make qubits out of this?

1. We need to trap the atoms
2. We need to identify a $|0\rangle$ and a $|1\rangle$ state
3. We need to be able to address transitions between $|0\rangle$ and $|1\rangle$
4. We need to be able to produce entanglement between the atoms
5. We need to be able to measure the state of the system

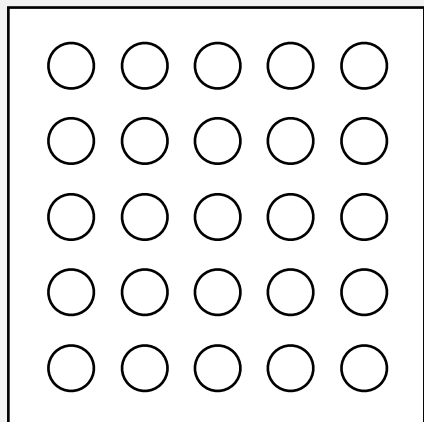
Most of these
are dependent
on each other

1. Trapping the atoms

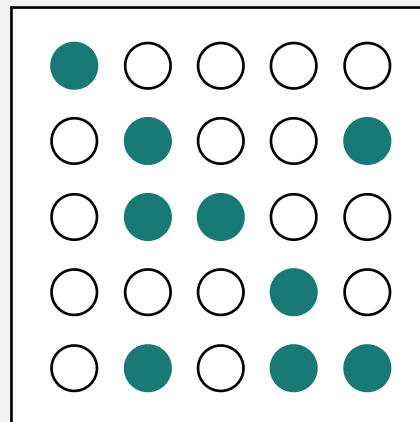
- ◉ We use optical tweezers to trap individual atoms in a region of around $1 \mu\text{m}$



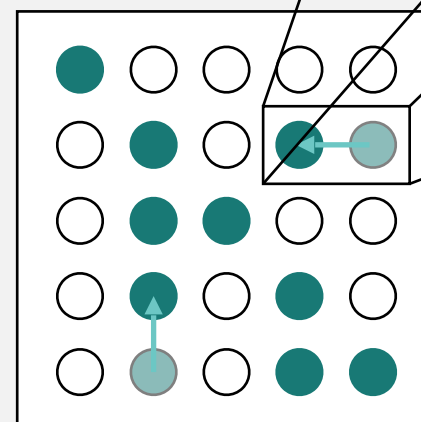
1. Trapping the atoms



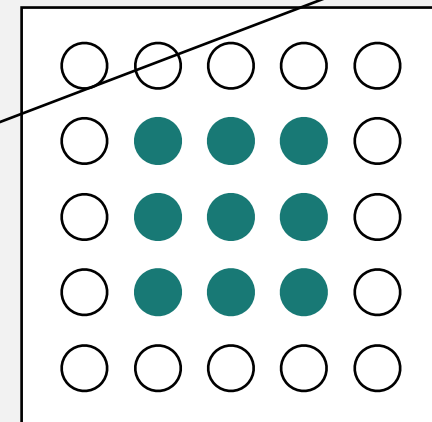
Prepare some traps



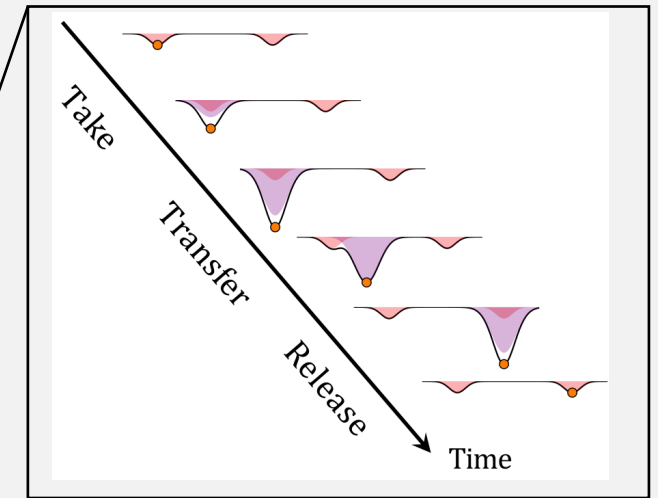
Load the traps randomly with Rubidium atoms



Rearrange the atoms by moving them to the desired trap

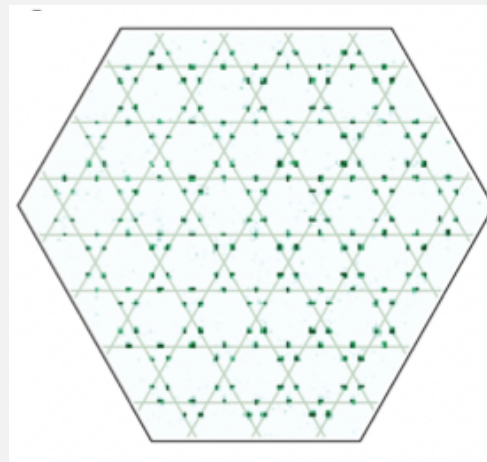


Final layout

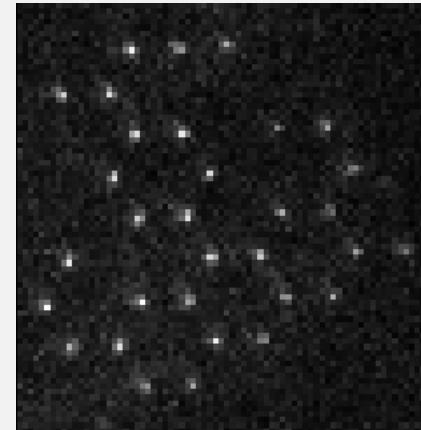


1. Trapping the atoms

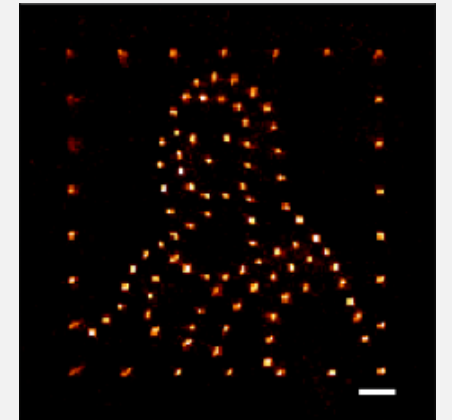
- High flexibility: atoms can be arranged in arbitrary fixed 2D configurations



<https://arxiv.org/abs/2104.04119>



<https://arxiv.org/abs/2211.16337>



<https://arxiv.org/abs/2011.06827>

1. Trapping the atoms

196



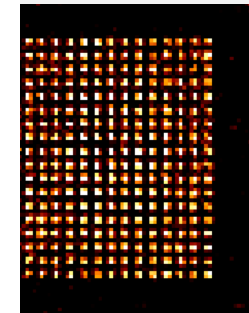
A tweezer array with 6100 highly coherent atomic qubits

Hannah J. Manetsch,^{*} Gyohei Nomura,^{*} Elie Bataille,^{*} Kon H. Leung, Xudong Lv, and Manuel Endres[†]
California Institute of Technology, Pasadena, CA 91125, USA

Optical tweezer arrays have had a transformative impact on atomic and molecular physics over the past years, and they now form the backbone for a wide range of leading experiments in quantum computing, simulation, and metrology. Underlying this development is the simplicity of single particle control and detection inherent to the technique. Typical experiments trap tens to hundreds of atomic qubits, and very recently systems with around one thousand atoms were realized without defining qubits or demonstrating coherent control. However, scaling to thousands of atomic qubits with long coherence times and low-loss, high-fidelity imaging is an outstanding challenge and critical for progress in quantum computing, simulation, and metrology, in particular, towards applications with quantum error correction. Here, we experimentally realize an array of optical tweezers trapping over 6,100 neutral atoms in around 12,000 sites while simultaneously surpassing state-of-the-art performance for several key metrics associated with fundamental limitations of the platform. Specifically, while scaling to such a large number of atoms, we also demonstrate a coherence time of 12.6(1) seconds, a record for hyperfine qubits in an optical tweezer array. Further, we show trapping lifetimes close to 23 minutes in a room-temperature apparatus, enabling record-high imaging survival of 99.98952(1)% in combination with an imaging fidelity of over 99.99%. Our results, together with other recent developments, indicate that universal quantum computing with ten thousand atomic qubits could be a near-term prospect. Furthermore, our work could pave the way for quantum simulation and metrology experiments with inherent single particle readout and positioning capabilities at a similar scale.



324



Chymik et al.

2014

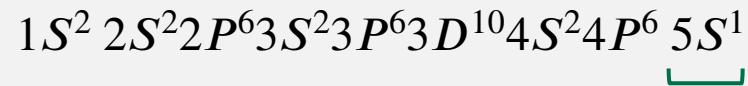
2016-2017

2020

2022

2. Making Qubits out of neutral atoms

We use as a $|0\rangle$ the ground state of Rubidium:



These are called Rydberg states



As a $|1\rangle$ state, we use a highly excited state, i.e. a state where the valence electron is in a level with high principal quantum number ($n \sim 70$)

$$\begin{aligned} \text{For } n = 60, \\ R \sim n^2 a_0 \rightarrow \sim 100 \text{ nm} \\ \tau \sim n^3 \rightarrow \sim 100 \mu\text{s} \end{aligned}$$

$$|0\rangle \rightarrow |5S\rangle$$

$$|0\rangle \rightarrow |5S\rangle$$

$$|0\rangle \rightarrow |5S\rangle$$

$$|1\rangle \rightarrow |60S\rangle$$

$$|1\rangle \rightarrow |70S\rangle$$

$$|1\rangle \rightarrow |70S\rangle$$

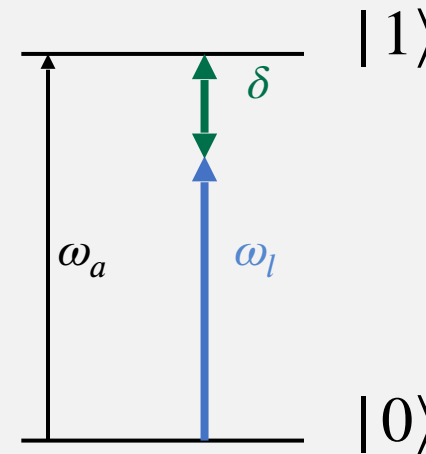
<https://arxiv.org/abs/2211.16337>

<https://arxiv.org/abs/2202.09372>

<https://arxiv.org/abs/1707.04344>

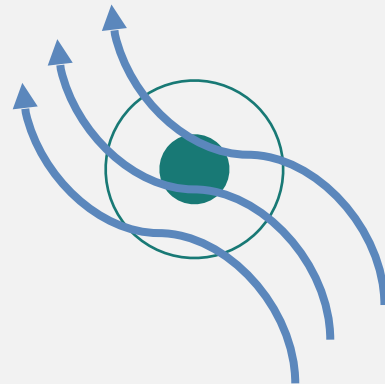
3. Addressing single qubit transition

- This is done by shining on the atom a laser beam very close to the transition energy between $|0\rangle$ and $|1\rangle$
- The difference between the resonant frequency ω_a and the laser frequency ω_l is called detuning, usually denoted δ

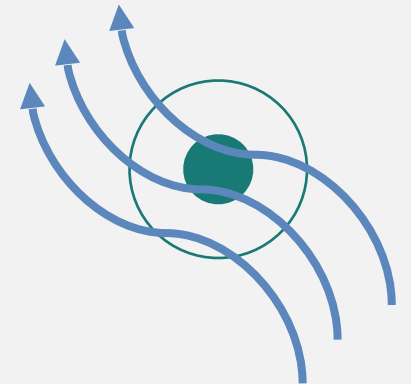


Entangling qubits

- two atoms in $|00\rangle$, far apart ($\geq 15\mu m$)



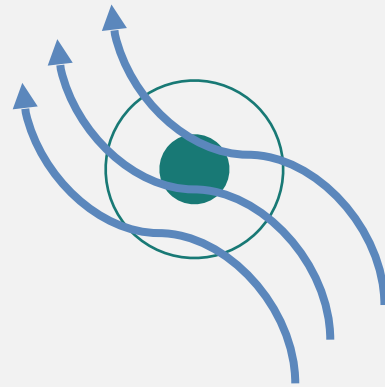
Laser resonant with the transition $|0\rangle$ to $|1\rangle$



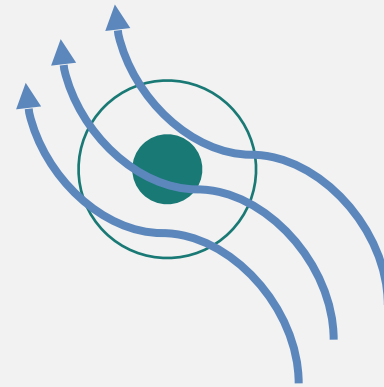
Laser resonant with the transition $|0\rangle$ to $|1\rangle$

Entangling qubits - Rydberg blockade

- We put the two atoms in $|00\rangle$, close to each other ($\sim 5,6\mu m$)
- When the resonant laser is switched on, we end up with the entangled state $|01\rangle + |10\rangle$ rather than $|11\rangle$



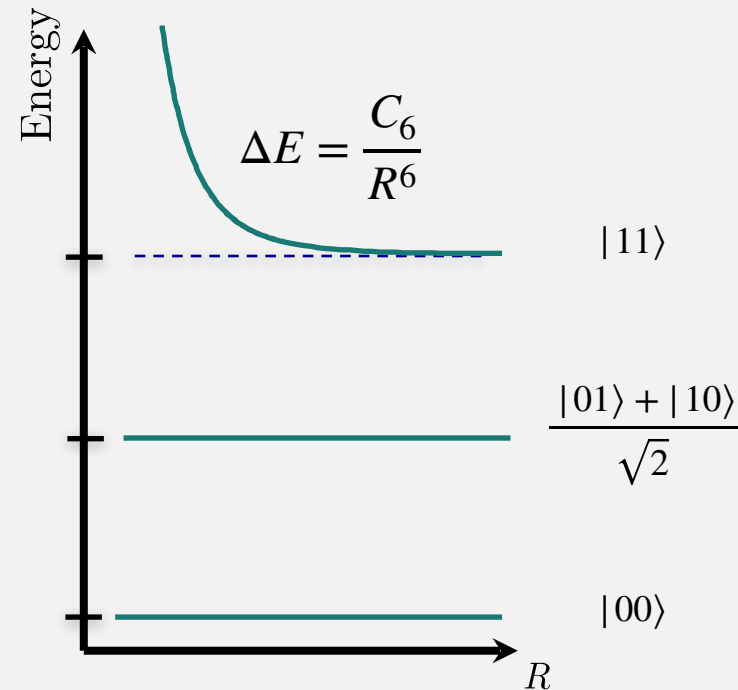
Laser resonant with the transition $|0\rangle$ to $|1\rangle$



Laser resonant with the transition $|0\rangle$ to $|1\rangle$

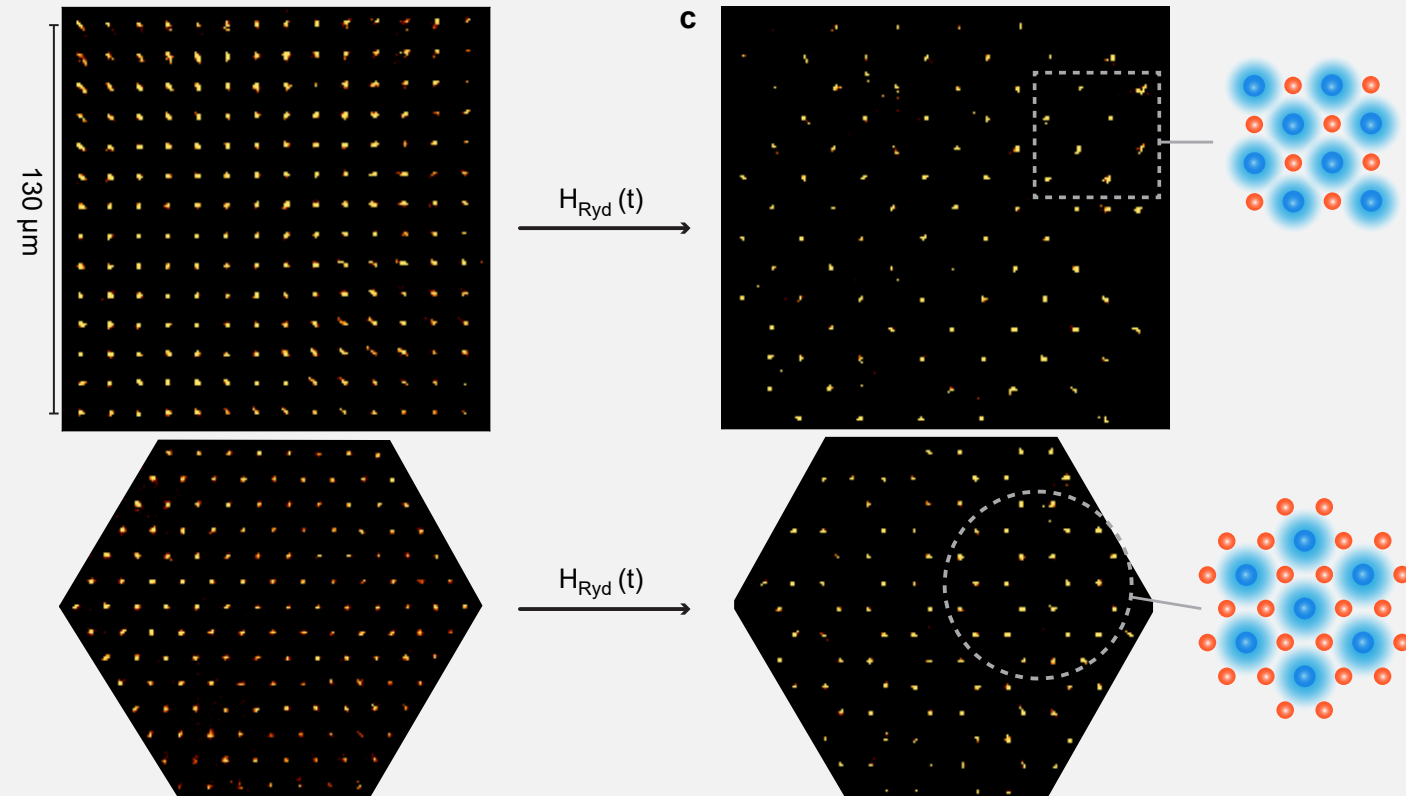
Entangling qubits - van der Waals interactions

- Two Rydberg states interact with a van der Waals interaction decaying as R^{-6} (with R distance between the atoms)
- The interaction shifts upwards the energy of the $|11\rangle$ level, favouring the excitation of the entangled state $|01\rangle + |10\rangle$ instead
- Importantly: during the measurement, we always observe states with Rydberg blockade



Measuring the qubits

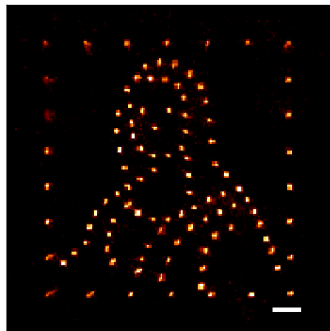
- The optical tweezer is actually repulsive for atoms in the $|1\rangle$ state and for that reason, during quantum computations, the tweezers are switched off.
- After the quantum evolution of the system, the tweezers are turned back on and atoms in $|1\rangle$ are expelled from the traps and lost, while atoms in $|0\rangle$ are recaptured
- A Fluorescent light is shone on the atoms, and the emission is captured by a CCD camera, which therefore only sees atoms in $|0\rangle$. The remaining spots are then assumed to be atoms in the state $|1\rangle$.



<https://arxiv.org/abs/2012.12268>

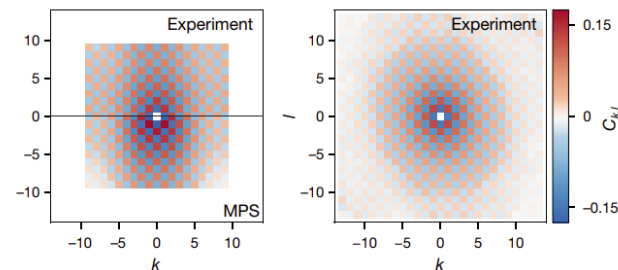
Rydberg atomic array for quantum simulation

Optical tweezers arrays allow for very flexible atomic register – can directly port amorphous materials into system



Adapted from Phys. Rev. A **102**, 063107

Scalable to hundreds of atoms – can capture both short-range order and lack of long-range order.



Adapted from Nature, **595**, 233–238 (2021)

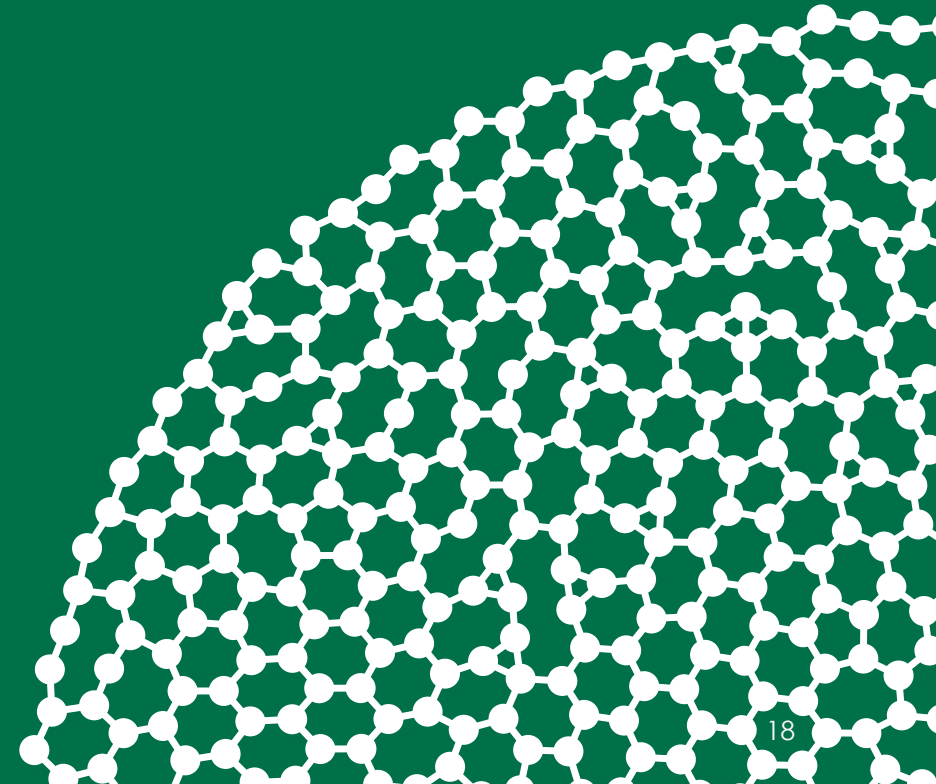
Can realise both the Ising model and XY model

$$\mathcal{H}(t) = \frac{\hbar}{2}\Omega(t) \sum_j \sigma_j^x - \hbar\delta(t) \sum_j n_j + \sum_{i \neq j} \frac{C_6}{r_{ij}^6} n_i n_j,$$

$$\mathcal{H}(t) = \frac{\hbar}{2}\Omega(t) \sum_j \sigma_j^x - \frac{\hbar}{2}\delta(t) \sum_j \sigma_j^z + 2 \sum_{i \neq j} \frac{C_3}{r_{ij}^3} (\sigma_i^x \sigma_j^x + \sigma_i^y \sigma_j^y).$$

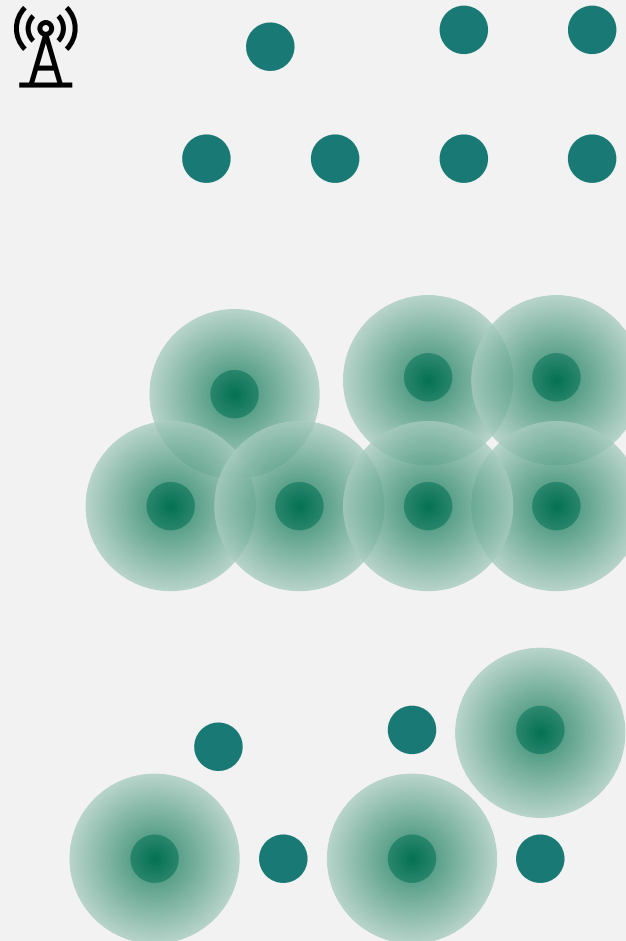
2

Maximum independent set



A first example: Placing antennas in cities

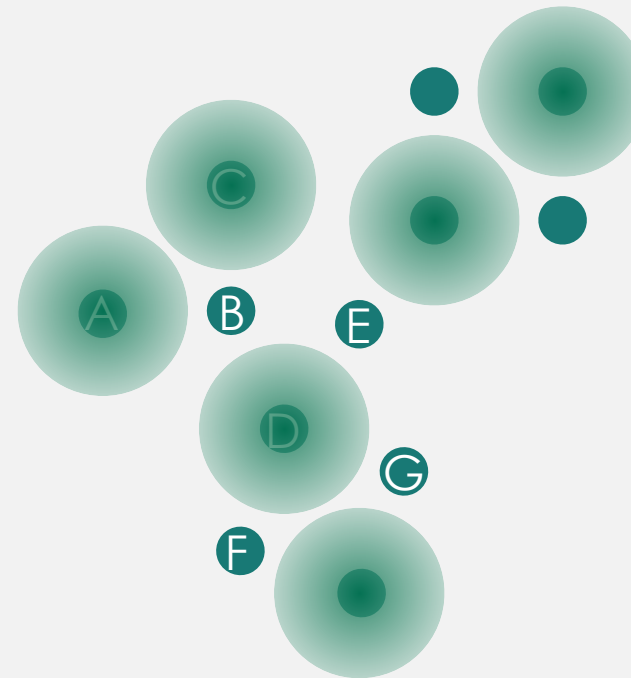
- ◉ We have to decide where to place antennas to maximise their coverage.
- ◉ Constraint: Two antennas should not interfere.
- ◉ Finding the maximum subset is the so called maximum independent set (MIS)
- ◉ Brute force: search within the 2^n sets



A second example: networking event

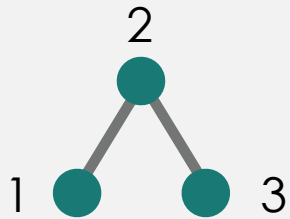
- You have a list of employees and their direct collaborators in the company.
- You want to organise an event
 - with a maximum employees
 - where none of the employees see their direct collaborators.

Alan	Bob			
Bob	Alan	Charline	Daniel	Eleanore
Daniel	Bob	Eleanore	Farid	Guy
...				



Graph theory

An **undirected graph** is a pair (V, E) where V is finite set $V = \{V_1, \dots, V_n\}$ (vertices), and E is a subset of $V \times V$ (edges).

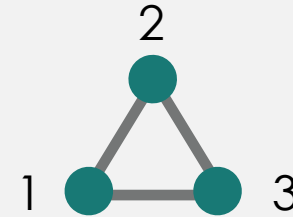


$$V = \{1, 2, 3\}$$

$$E = \{(1, 2), (2, 3)\}$$

$$A = \begin{pmatrix} 0 & 1 & 0 \\ 1 & 0 & 1 \\ 0 & 1 & 0 \end{pmatrix}$$

An **adjacency matrix** is a square matrix used to represent a finite graph. The elements of the matrix indicate whether pairs of vertices are adjacent or not in the graph.



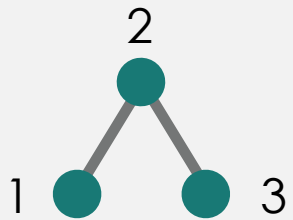
$$V = \{1, 2, 3\}$$

$$E = \{(1, 2), (2, 3), (3, 1)\}$$

$$A = \begin{pmatrix} 0 & 1 & 1 \\ 1 & 0 & 1 \\ 1 & 1 & 0 \end{pmatrix}$$

Graph theory

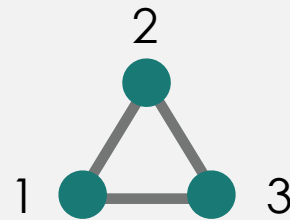
An independent set of a graph $G = (V, E)$ is a subset $S \subset V$ such that no pair of vertices in S is connected by an edge.



$$V = \{1, 2, 3\}$$

$$E = \{(1, 2), (2, 3)\}$$

$$A = \begin{pmatrix} 0 & 1 & 0 \\ 1 & 0 & 1 \\ 0 & 1 & 0 \end{pmatrix}$$

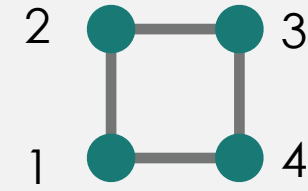


$$V = \{1, 2, 3\}$$

$$E = \{(1, 2), (2, 3), (3, 1)\}$$

$$A = \begin{pmatrix} 0 & 1 & 1 \\ 1 & 0 & 1 \\ 1 & 1 & 0 \end{pmatrix}$$

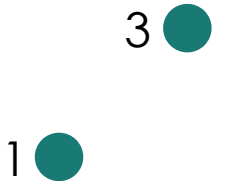
$$V_1, V_2 \in S \Rightarrow (V_1, V_2) \notin E$$



$$V = \{1, 2, 3, 4\}$$

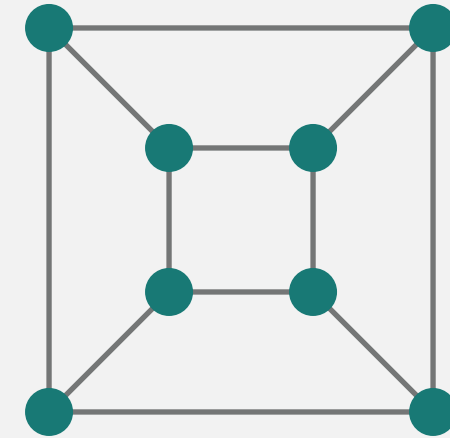
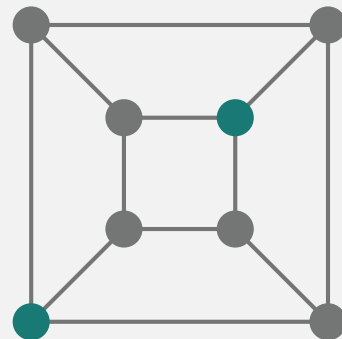
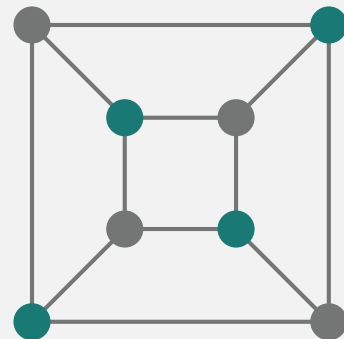
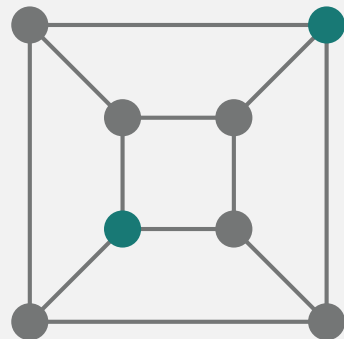
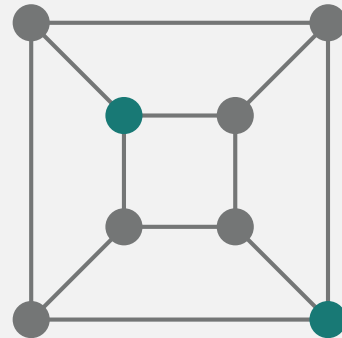
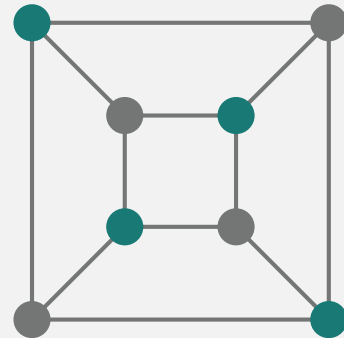
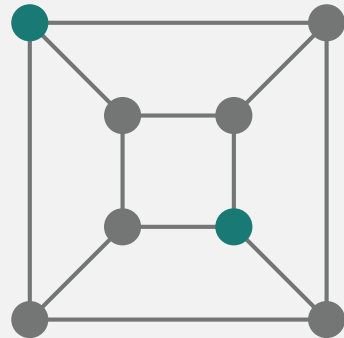
$$E = \{(1, 2), (2, 3), (3, 4), (4, 1)\}$$

$$A = \begin{pmatrix} 0 & 1 & 0 & 1 \\ 1 & 0 & 1 & 0 \\ 0 & 1 & 0 & 1 \\ 1 & 0 & 0 & 1 \end{pmatrix}$$



Graph theory

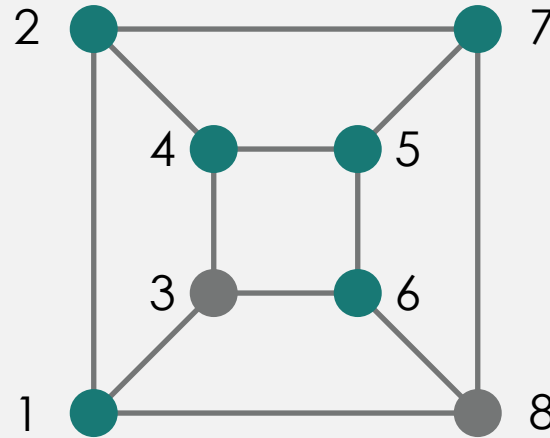
A Maximum independent set of a graph G is a subset S of V which is an independent set, and it has the maximum cardinality among all possible independent sets



1. Find all the independent set for this graph.
2. Find the maximum independent set(s).

Boolean reformulation

- We give an index to the vertices of the graph.
- A subset S can also be defined in a boolean manner
 - 1 if in the subset
 - 0 if not in the subset
- We want to maximise the cardinality of the subset $\#S$.
- The independent set constraint can be rewritten as $h(S) = 0$.



$$\{3,8\} \longrightarrow S = (00100001)$$

$$\text{Size of the set: } f(S) = \sum_{i \in V} n_i^{(S)} = \#S$$

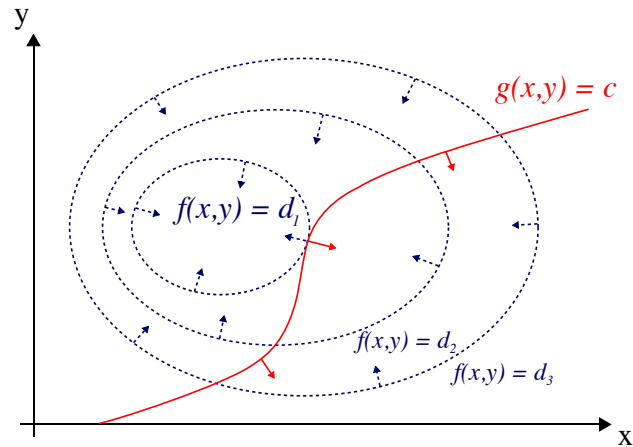
$$\text{IS condition: } h(S) = \sum_{i,j \in E} n_i^{(S)} n_j^{(S)} = 0$$

BOOLEAN REFORMULATION OF THE MIS

$$\begin{aligned} & \max_{S \in \mathcal{B}} f(S) \\ & \text{s.t. } h(S) = 0 \end{aligned}$$

MIS as an unconstrained optimisation problem

LAGRANGE MULTIPLIERS



Given the problem

$$\max_x f(x) \text{ s.t. } h(x) = 0,$$

We define the Lagrangian

$$\mathcal{L}(x) = f(x) + \lambda h(x)$$

The solution of the constrained optimisation problem will be a saddle point of \mathcal{L} .

$$\partial_\lambda \mathcal{L} = 0 \text{ and } \partial_x \mathcal{L} = 0$$

$$g(x) = 0 \text{ and } \partial_x f + \lambda \partial_x g = 0$$

MIS as an unconstrained optimisation problem

- We therefore want to minimise $C = -\mathcal{L}$.
- In principle, the minimisation should be both on S and on λ
- Since $h(S) \geq 0$, the first term always favours IS solutions.
- The proper choice of λ can be done through an optimisation procedure.
- One can show that for $\lambda > 1$, the solution is **always an IS** (see e.g. appendix of 2006.11190)
- We have now reduced our MIS to a QUBO problem and also a problem that can be natively solved on the QPU.
- We will now see how one can reach the ground state of the optimisation problem with quantum annealing.

$$\begin{aligned}
 C &= \min_{S \in \mathcal{B}} \lambda h(S) - f(S) \\
 &= \min_{S \in \mathcal{B}} \lambda \sum_{i,j \in V} n_i^{(S)} n_j^{(S)} - \sum_{i \in V} n_i^{(S)} \\
 &\quad \geq 0
 \end{aligned}$$

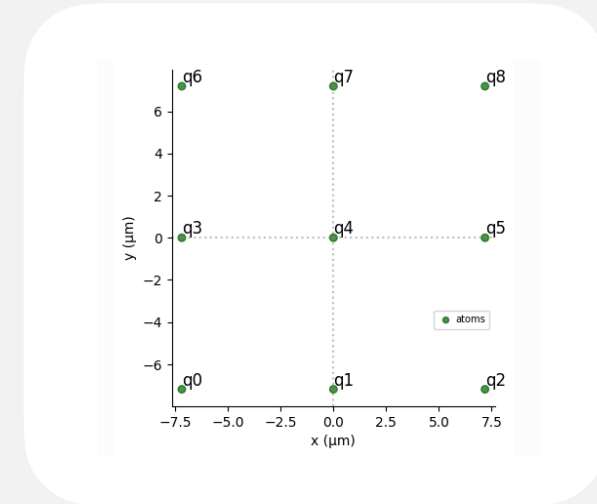
Quantum evolution on a QPU

- Initially ($t = 0$) all the spins are in the GS. $|00 \dots 00\rangle$.

- A run consists on modulating

$$H_{\text{pulse}} = \frac{\hbar}{2} \sum_i \sin(\phi)\Omega(t)\sigma_i^x - \cos(\phi)\Omega(t)\sigma_i^y - \delta(t)\sigma_i^z.$$

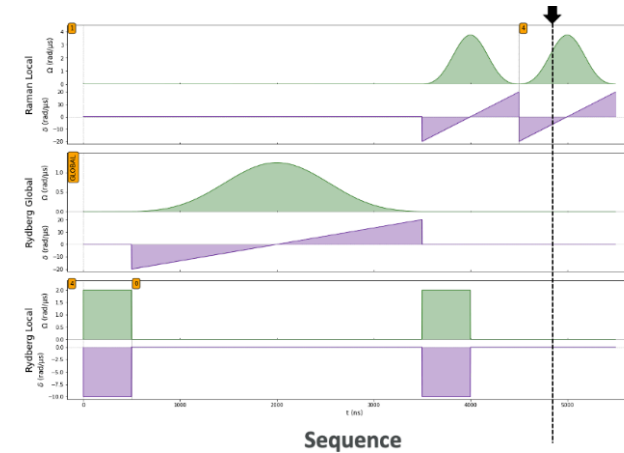
- Pulse shaping is possible (interpolated waveform), but with a certain modulation bandwidth.
- The use of an Electro Optical Modulator (EOM) allows one to achieve square pulses with high precision.
- Maximal allowed time before decoherence starts to matter is typically $\tau_{\text{max}} = 4 \mu\text{s}$.



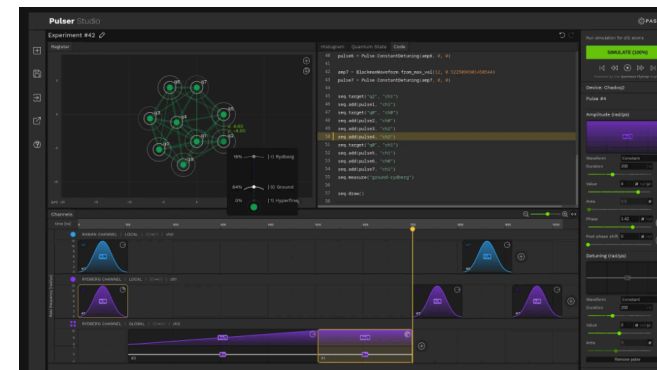
Open source emulator

- ◉ Play with analog device specs.
- ◉ Simulate realistic pulse shapes.
- ◉ EOM, addressability, ...
- ◉ State preparation, shot noise, ...

Pulser



Pulser Studio



Quantum evolution: A review

- Initially ($t = 0$) all the spins are in the GS $|0\rangle \equiv |00 \dots 00\rangle$.
- Quantum evolution under the time-dependent Hamiltonian

$$H = \hbar \sum_i \frac{\Omega(t)}{2} \sigma_i^x - \delta(t) n_i + \sum_{i \neq j} V_{ij} n_i n_j$$

- A time t , the state is described by

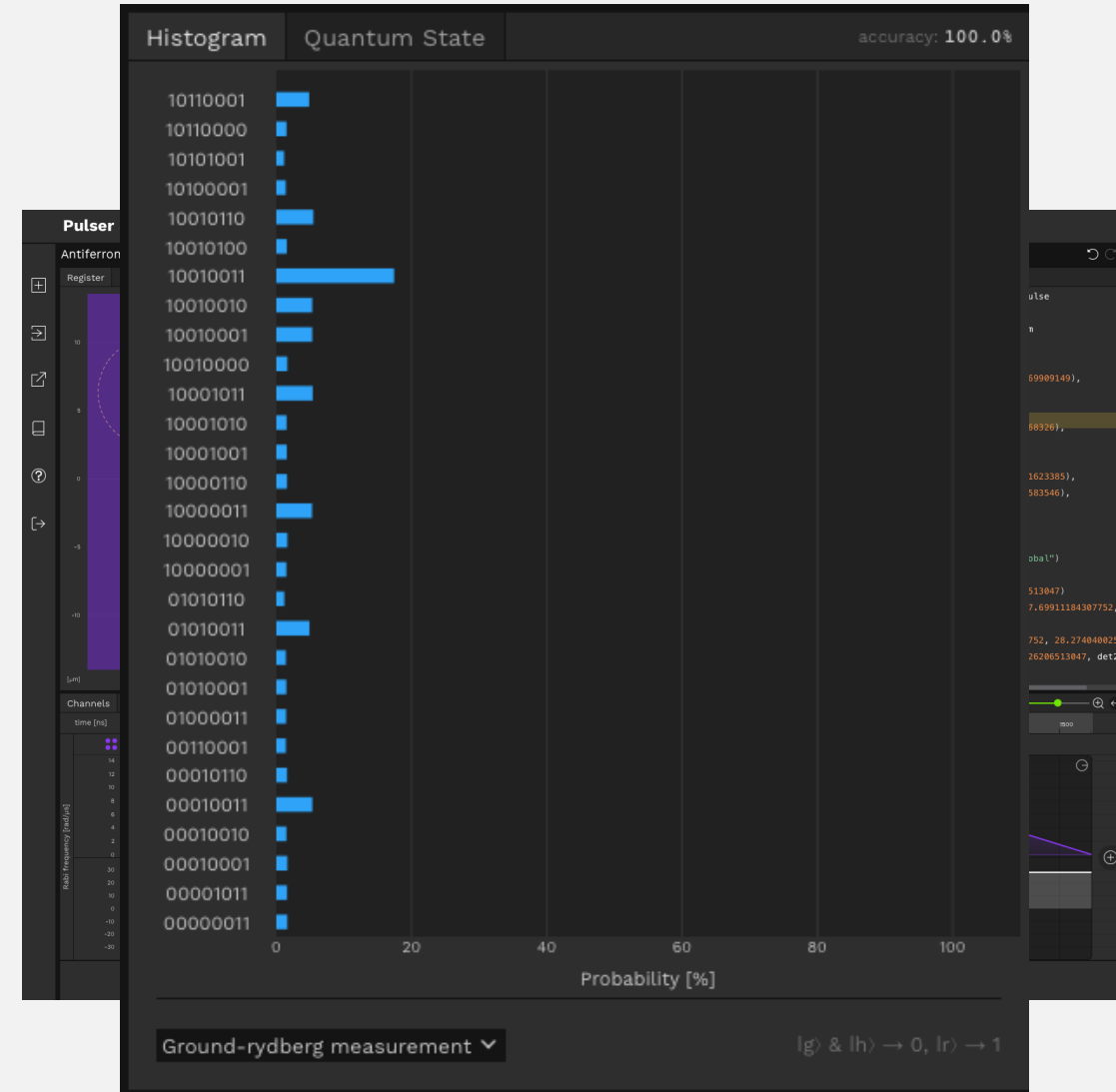
$$|\psi(t)\rangle = \exp^{-i \int_0^t H(t) dt} |0\rangle$$

- It is also worth to write $|\psi(t)\rangle$ in the computational basis

$$|\psi(t)\rangle = \sum_{S \in \mathcal{B}} a_S(t) |S\rangle$$

- The probability of measuring a given bitstring S' is then given by

$$P(S') = |\langle S' | \psi(t) \rangle|^2 = |a_{S'}|^2$$



Quantum evolution: Rabi oscillations

Let us consider the single qubit Hamiltonian

$$H = \Omega\sigma_x + \delta\sigma_z$$

- Compute the time-evolution of the initial state $|\psi_0\rangle = |0\rangle$.
- Compute the probability $P(1)$

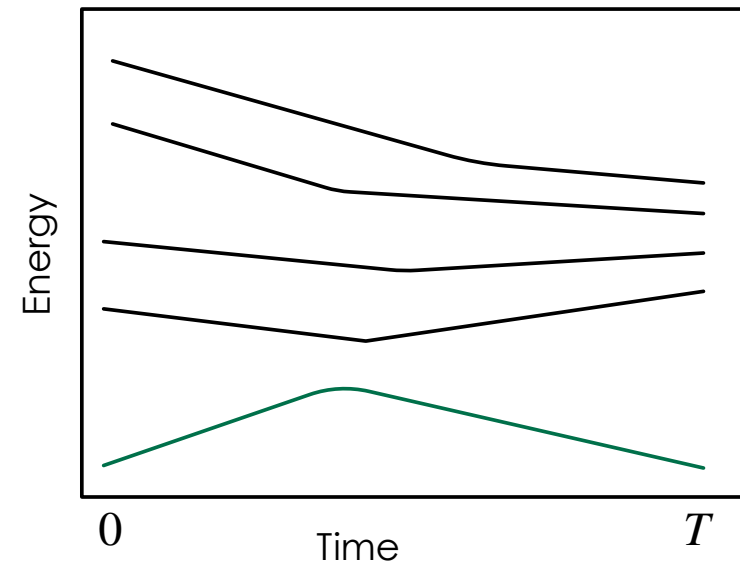
Quantum annealing

- Let us assume we know the ground state at time 0 of an Hamiltonian H_0 and we do not know the ground state of the Hamiltonian H_1 .
- For a sufficient slow evolution, we can drive continuously the system from the initial state to the final state, while staying in the instantaneous GS.
- This allows then to connect adiabatically the initial GS to the final GS.
- Important condition:** there should be a gap between the instantaneous GS and the first excited state.
- If we are not adiabatic, then this can lead to transitions to excited states
- Example:** Landau Zener transitions \rightarrow exponentially decaying in terms of a ratio between the gap and the velocity of the path.

QUANTUM ANNEALING

$$H(t) = (T - t) H_0 + t H_1$$

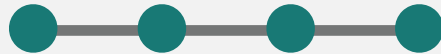
$$|\psi(t)\rangle = e^{\int_0^t H(t) dt} |\psi(0)\rangle$$



A first example of MIS

Let us consider the antenna problem on a line with 4 sites

- Analyse the problem by the brute force method
- Reformulate the MIS problem as a QUBO problem
- Compute the value of \mathcal{L}
- What happens for $\lambda \ll 1$?



First example of MIS: quantum annealing

Probing many-body dynamics on a 51-atom quantum simulator

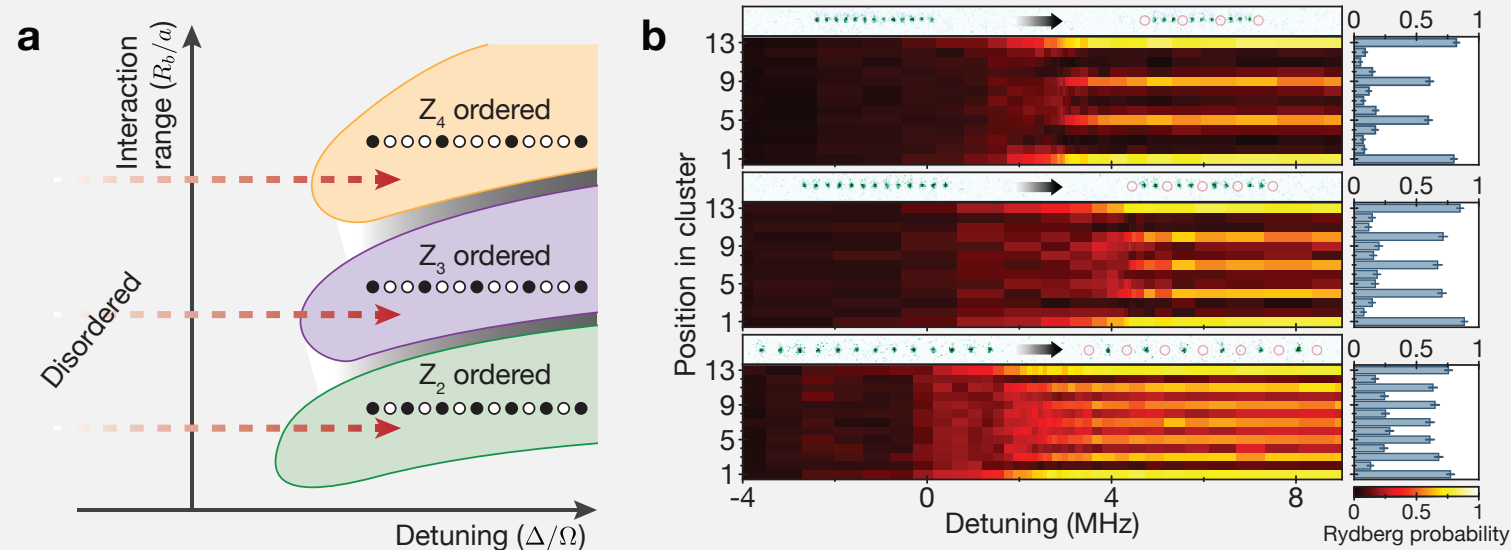
Hannes Bernien,¹ Sylvain Schwartz,^{1,2} Alexander Keesling,¹ Harry Levine,¹ Ahmed Omran,¹ Hannes Pichler,^{3,1} Soonwon Choi,¹ Alexander S. Zibrov,¹ Manuel Endres,⁴ Markus Greiner,¹ Vladan Vuletić,² and Mikhail D. Lukin¹

¹Department of Physics, Harvard University, Cambridge, MA 02138, USA

²Department of Physics and Research Laboratory of Electronics, Massachusetts Institute of Technology, Cambridge, MA 02139, USA

³Institute for Theoretical Atomic, Molecular and Optical Physics, Harvard-Smithsonian Center for Astrophysics, Cambridge, MA 02138, USA

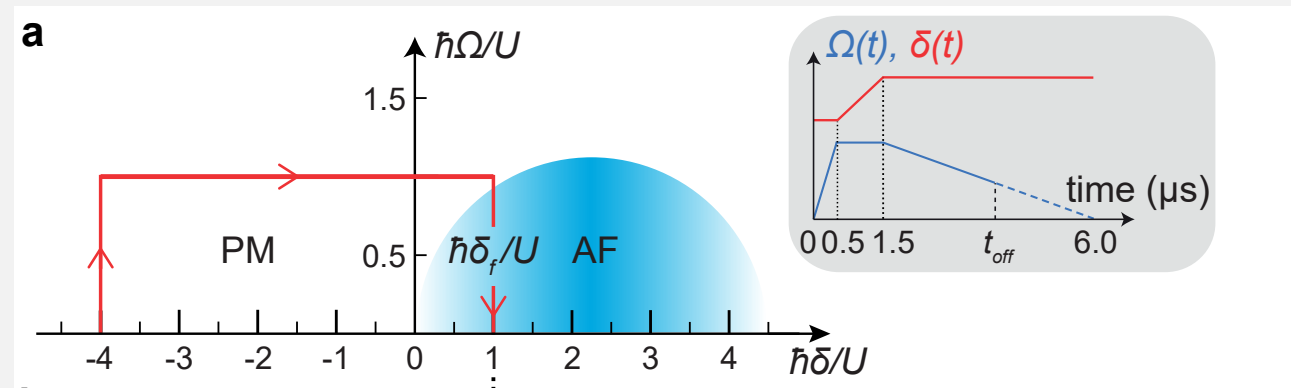
⁴Division of Physics, Mathematics and Astronomy, California Institute of Technology, Pasadena, CA 91125, USA



H. Bernien et al, Nature 551, 579-584 (2017)

Optimising the pulse sequence

- We have to choose the path of the quantum annealing
- First approach: linear ramps.
- This might not be optimal.
- **Remember:** Small gaps and potential gap closing \rightarrow transitions to excited states
- **Other approach:** We aim to minimise a cost function.
- In our case, the energy of the spin system, which corresponds to the Lagrangian \mathcal{L} is the the function we want to minimize.



<https://arxiv.org/abs/2012.12268>

Expectation values on the QPU

- We perform the time evolution on the QPU
- We should then measure the expectation value of the energy

$$E = \langle \psi(T) | H | \psi(T) \rangle,$$

$$\text{where } H = -\delta(T) \sum_i n_i + \sum_{i \neq j} V_{ij} n_i n_j.$$

- In the computational basis

$$|\psi(t)\rangle = \sum_{S \in \mathcal{B}} a_S(t) |S\rangle,$$

$$E = -\delta(T) \sum_{S \in \mathcal{B}, i} |a_S(T)|^2 \langle S | n_i | S \rangle + V_{ij} \sum_{S, \in \mathcal{B}, i, j} |a_S(T)|^2 \langle S | n_i n_j | S \rangle$$

- Recall that n_i is diagonal in the computational basis

Experimental implementation

RESEARCH

QUANTUM SIMULATION

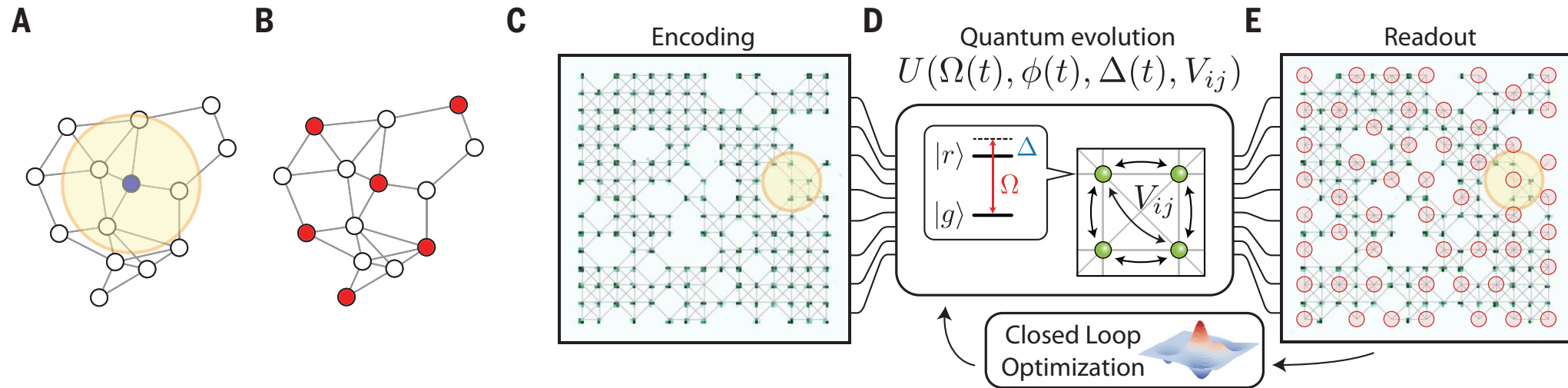
Quantum optimization of maximum independent set using Rydberg atom arrays

S. Ebadi^{1†}, A. Keesling^{1,2†}, M. Cain^{1†}, T. T. Wang¹, H. Levine^{1‡}, D. Bluvstein¹, G. Semeghini¹, A. Omran^{1,2}, J.-G. Liu^{1,2}, R. Samajdar¹, X.-Z. Luo^{2,3,4}, B. Nash⁵, X. Gao¹, B. Barak⁵, E. Farhi^{6,7}, S. Sachdev^{1,8}, N. Gemelke², L. Zhou^{1,9}, S. Choi⁷, H. Pichler^{10,11}, S.-T. Wang², M. Greiner^{1*}, V. Vuletić^{12*}, M. D. Lukin^{1*}

Realizing quantum speedup for practically relevant, computationally hard problems is a central challenge in quantum information science. Using Rydberg atom arrays with up to 289 qubits in two spatial dimensions, we experimentally investigate quantum algorithms for solving the maximum independent set problem. We use a hardware-efficient encoding associated with Rydberg blockade, realize closed-loop optimization to test several variational algorithms, and subsequently apply them to systematically explore a class of graphs with programmable connectivity. We find that the problem hardness is controlled by the solution degeneracy and number of local minima, and we experimentally benchmark the quantum algorithm's performance against classical simulated annealing. On the hardest graphs, we observe a superlinear quantum speedup in finding exact solutions in the deep circuit regime and analyze its origins.

See also
arXiv:1808.10816 for the theory

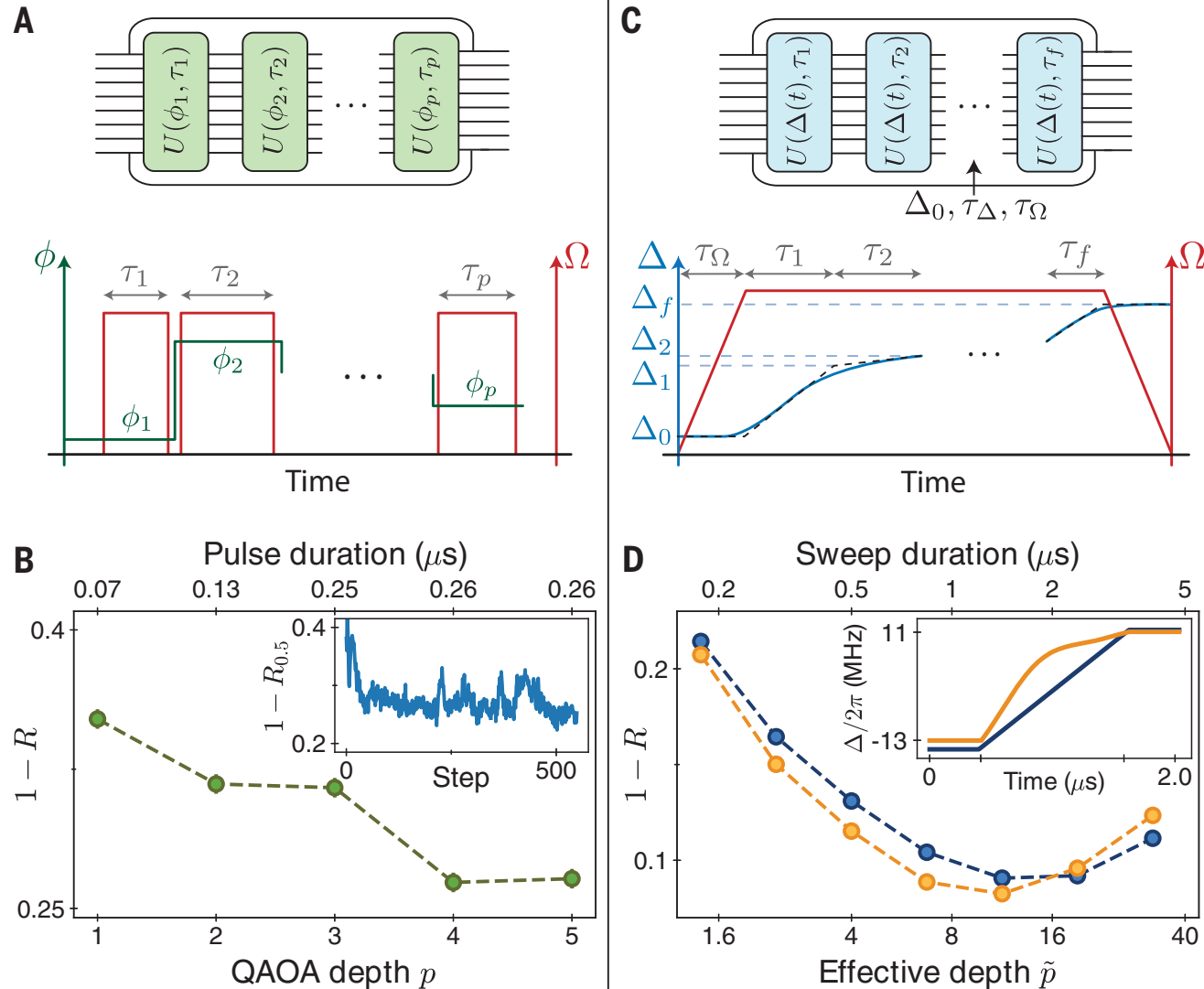
Experimental implementation



$$H_q = \frac{\hbar}{2} \sum_i \left[\Omega(t) e^{i\phi(t)} |0\rangle_i \langle 1| + \text{h.c.} \right],$$

$$H_{\text{cost}} = -\hbar\Delta(t) \sum_i n_i + \sum_{i<j} V_{ij} n_i n_j$$

Experimental implementation

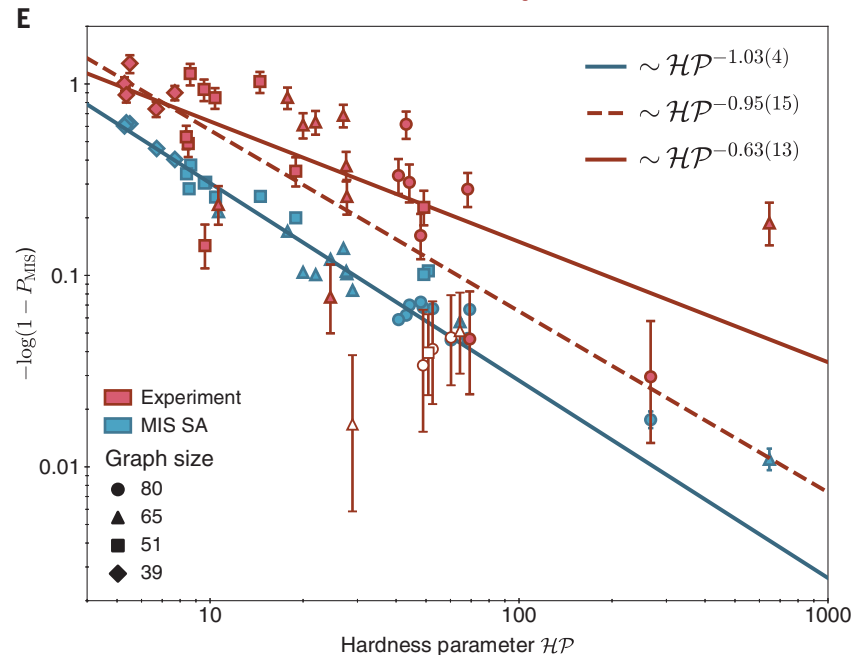
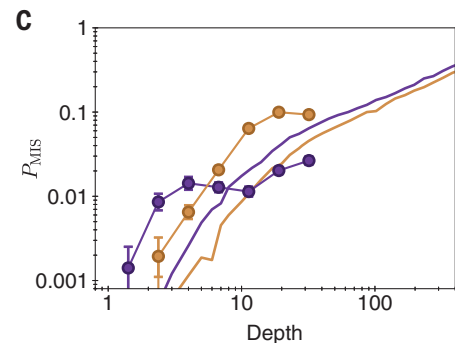
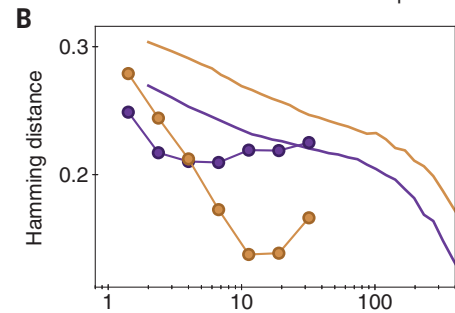
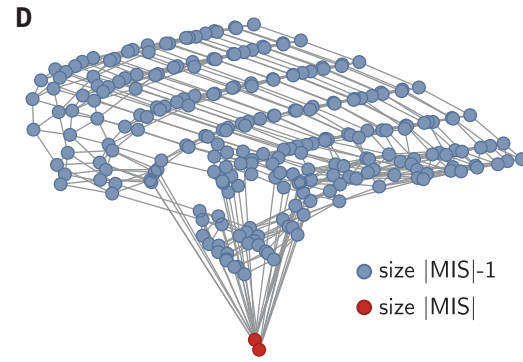
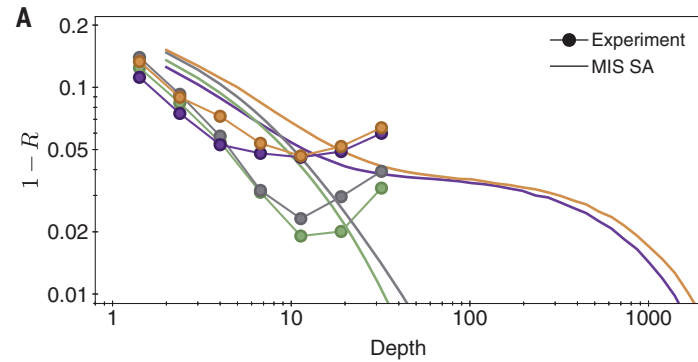


$$H_q = \frac{\hbar}{2} \sum_i \left[\Omega(t) e^{i\phi(t)} |0\rangle_i \langle 1| + \text{h.c.} \right],$$

$$H_{\text{cost}} = -\hbar \Delta(t) \sum_i n_i + \sum_{i < j} V_{ij} n_i n_j$$

$$R = \sum_i \langle \psi_f | n_i | \psi_f \rangle / \# \text{MIS}$$

Experimental implementation



first excited states

$$HP = \frac{D_{|MIS|-1}}{|MIS| D_{|MIS|}}$$

MIS (or in our notation $f(S)$)

Quantum simulation vs classical numerics

Hardness of the Maximum Independent Set Problem on Unit-Disk Graphs and Prospects for Quantum Speedups

Ruben S. Andrist,^{1,*} Martin J. A. Schuetz,^{1,2,*} Pierre Minssen,^{3,*} Romina Yalovetzky,^{3,*} Shouvanik Chakrabarti,³ Dylan Herman,³ Niraj Kumar,³ Grant Salton,^{1,2,4} Ruslan Shaydulin,³ Yue Sun,³ Marco Pistoia,^{3,†} and Helmut G. Katzgraber^{1,†}

¹*Amazon Quantum Solutions Lab, Seattle, Washington 98170, USA*

²*AWS Center for Quantum Computing, Pasadena, CA 91125, USA*

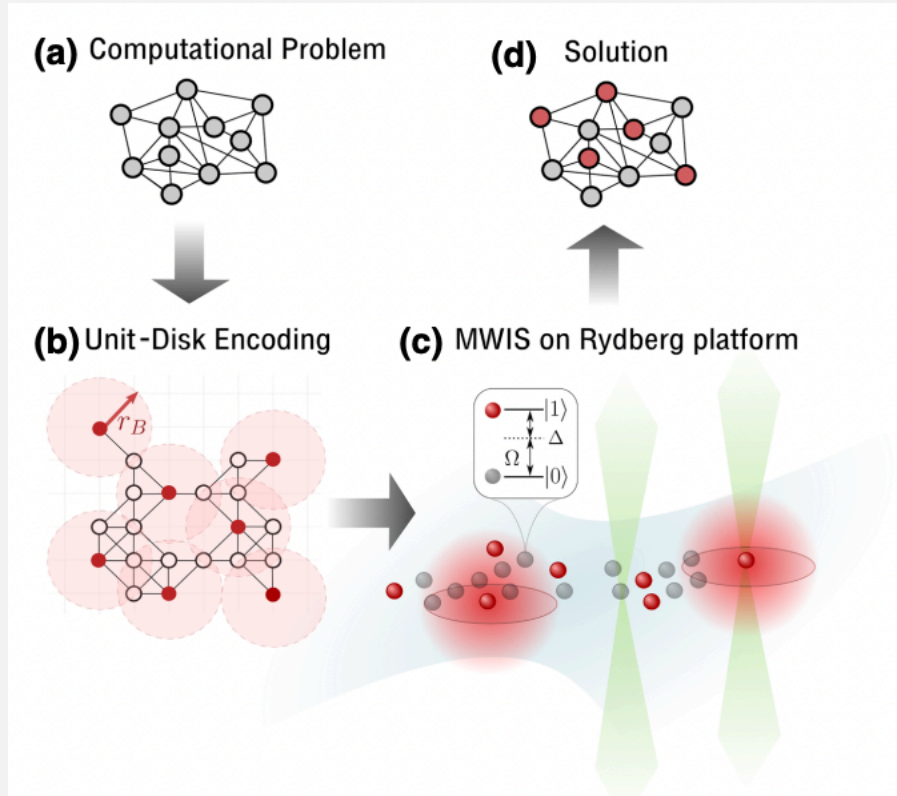
³*Global Technology Applied Research, JPMorgan Chase, New York, NY 10017 USA*

⁴*California Institute of Technology, Pasadena, CA, USA*

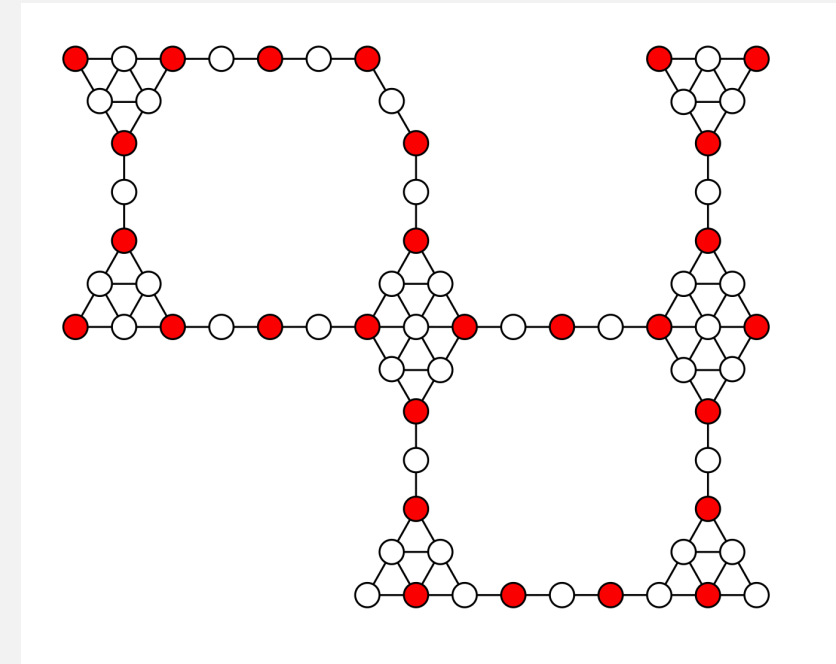
(Dated: July 19, 2023)

Rydberg atom arrays are among the leading contenders for the demonstration of quantum speedups. Motivated by recent experiments with up to 289 qubits [Ebadi *et al.*, Science **376**, 1209 (2022)] we study the maximum independent set problem on unit-disk graphs with a broader range of classical solvers beyond the scope of the original paper. We carry out extensive numerical studies and assess problem hardness, using both exact and heuristic algorithms. We find that quasi-planar instances with Union-Jack-like connectivity can be solved to optimality for up to thousands of nodes within minutes, with both custom and generic commercial solvers on commodity hardware, without any instance-specific fine-tuning. We also perform a scaling analysis, showing that by relaxing the constraints on the classical simulated annealing algorithms considered in Ebadi *et al.*, our implementation is competitive with the quantum algorithms. Conversely, instances with larger connectivity or less structure are shown to display a time-to-solution potentially orders of magnitudes larger. Based on these results we propose protocols to systematically tune problem hardness, motivating experiments with Rydberg atom arrays on instances orders of magnitude harder (for established classical solvers) than previously studied.

Beyond MIS with analog **neutral atoms**



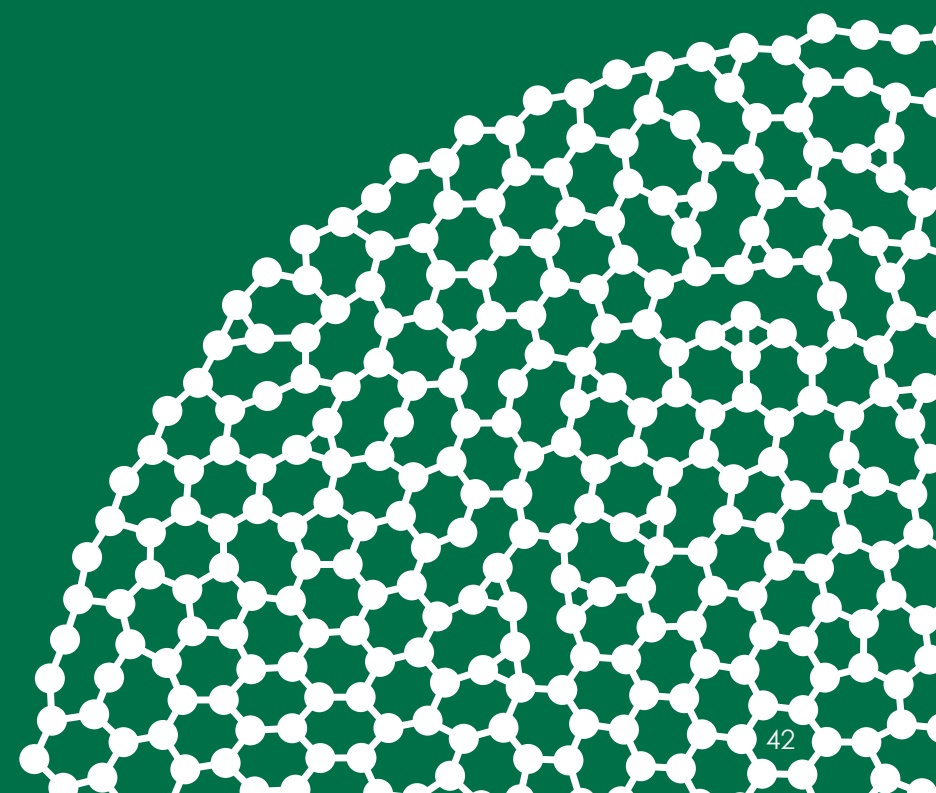
Nguyen, Minh-Thi, et al. "Quantum optimization with arbitrary connectivity using rydberg atom arrays." *PRX Quantum* 4.1 (2023): 010316.



M. Lanthaler, C. Daska, K. Ender, and W. Lechner, "Rydberg-blockade-based parity quantum optimization," *Physical Review Letters*, vol. 130, no. 22, p. 220601, 2023.

3

Amorphous quantum magnets

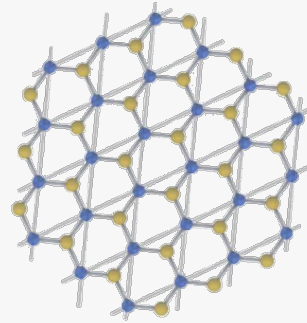


From crystals to amorphous solids

The disordered structure of the material makes it difficult to simulate and requires large approximations.

However, amorphous materials are ubiquitous and simulate them could lead to groundbreaking discoveries

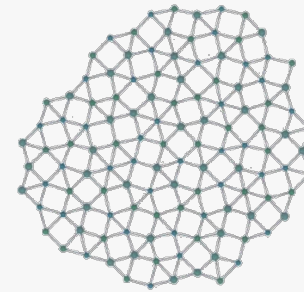
3 TYPES OF MATERIALS



Crystal lattice

Translational invariance

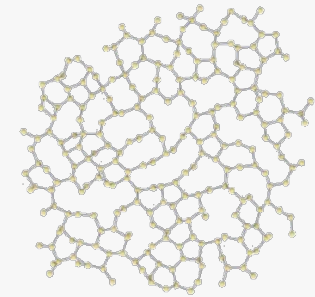
- These materials are *fully ordered and translational symmetry*
- Majority of quantum simulation results consider such lattice structures



Quasicrystal

Materials with no translational symmetry but long range order

- Proposal and first results for the quantum simulation with cold atoms



Amorphous materials

Short range order but *no long-range order*

- The quantum simulation of these is focus of this talk

Amorphous: Disordered at Long range and short ranged ordered

Amorphous materials have **no long-range order**

However, they have well defined **short-range order** due to covalent bonds: *bond lengths* and *bond angles*

The combination of these leads to a *well-defined coordination number*

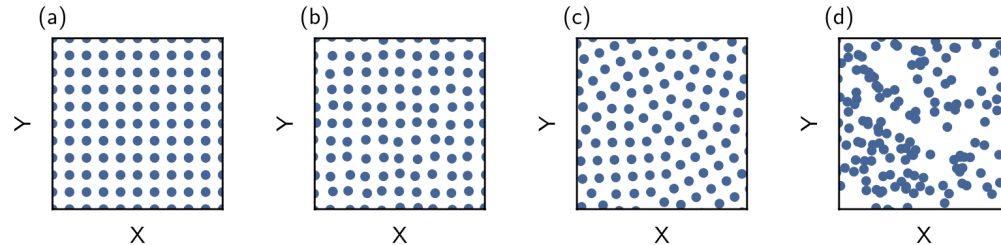
Reflected through in

- the **radial distribution function** $g(r)$

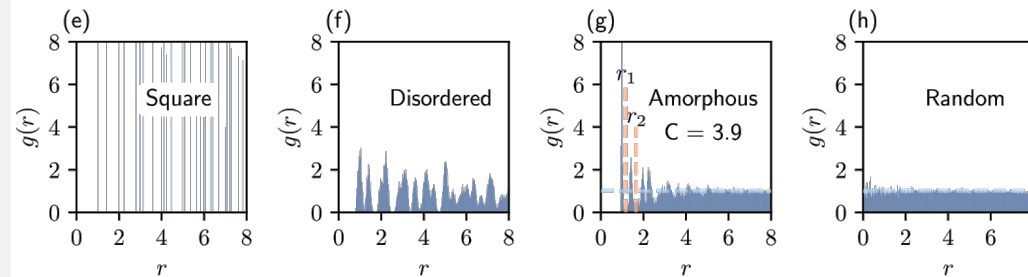
Coordination number

$$C = 2\pi \int_0^{R_1} r g(r) dr$$

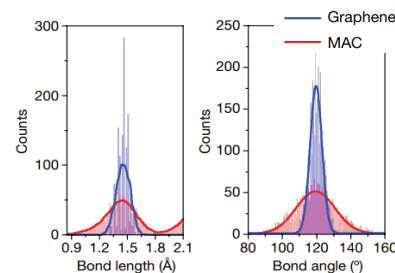
FROM ORDERED TO DISORDERED MATERIALS



RADIAL DISTRIBUTION FUNCTION

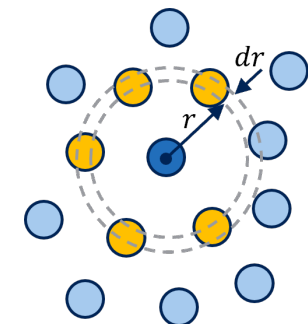


BOND LENGTHS AND BOND ANGLES IN GRAPHENE AND MONOLAYER AMORPHOUS CARBON

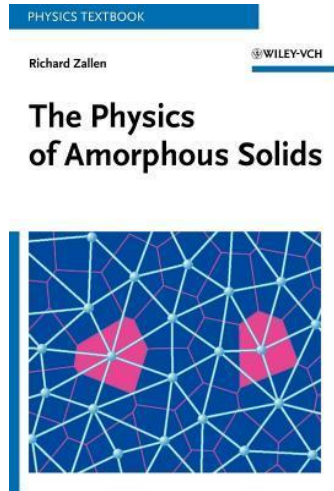


Adapted from *Nature*, **577**, 199–203 (2020)

$g(r)$: ATOMIC DENSITY FROM A REFERENCE ATOM

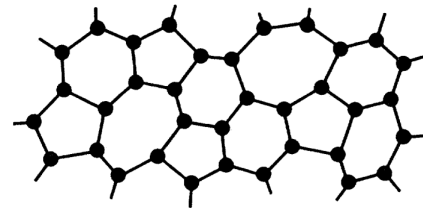


Interest in amorphous solids

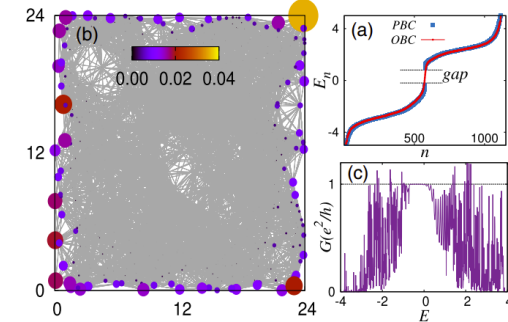


'Nearly all materials can, if cooled fast enough and far enough, be prepared as amorphous solids.'

Spectral gaps in DOS
 → *Amorphous Semiconductors*
 Phys. Rev. B 4, 2508



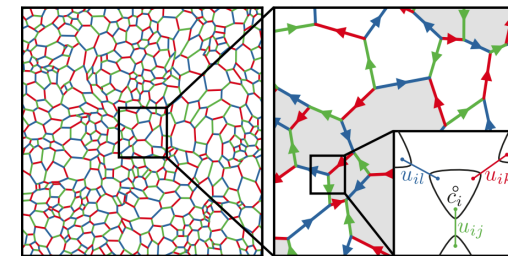
Amorphous Topological Insulators
 Phys. Rev. Lett. 118, 236402



Amorphous Superconductors
 Amorphous Superconductors,
 Tsuei, C.C. (1981).

Element \ Supercond. T _c	Crystal	Amorphous
Bi	5 mK	6 K
Be	26 mK	10 K
Al	1.18 K	6 K

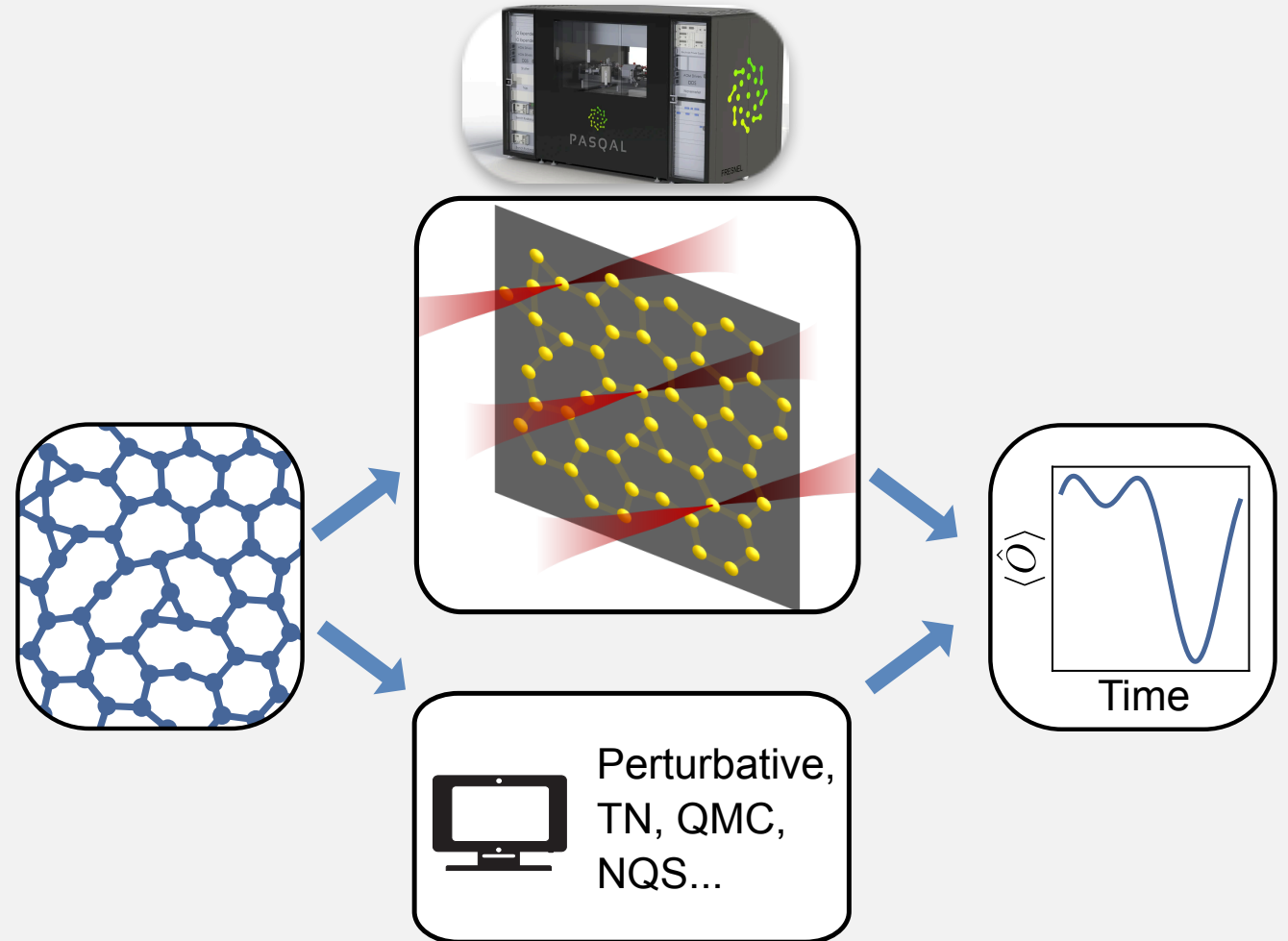
Adapted from Paul Corbae *et al* 2023 *EPL* 142 16001



Amorphous Quantum Spin Liquids
 Nat. Commun. 14, 6663 (2023)

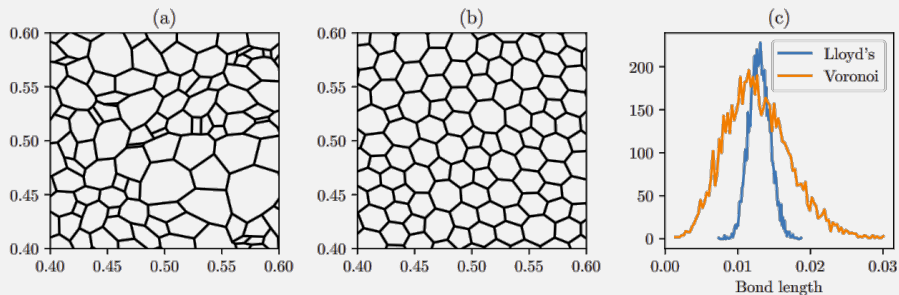
Amorphous Quantum Magnets

- much research into amorphous materials typically focusing on classical/non-interacting
- Limited research into work on quantum amorphous materials due to inherent complexity
 - inherent requirement of large systems
 - No translational symmetry



Amorphous solid Generation

Most common methods in previous literature is
Voronoi tessellation

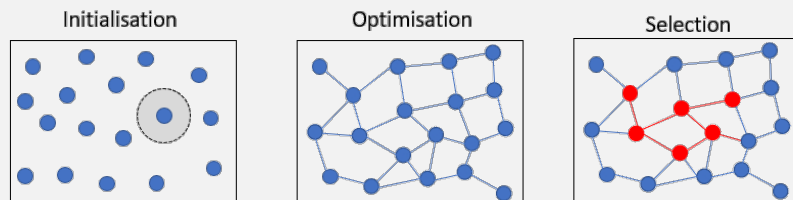


Adapted from *Nature* **volume 577**, 199–203 (2020)

Problems:

- Two sites connected by an edge (no matter its length) become nearest-neighbours.
- Limited control over coordination number and edge lengths – we consider $I \propto 1/r^6$

➤ We need a method with very precise control – use variational approach



$$\mathcal{L} = a_1 \sum_j \left| \sum_i k(r_{ij}) - m_j \right|^2 + a_2 \sum_{ij} \left(1 - \frac{1}{1 + e^{-\gamma(r_{ij} - r_{\min})}} \right) + a_2 \sum_{ij} \frac{e^{r_{ij} - r_{\max}}}{1 + e^{-\beta(r_{ij} - r_{\max})}}$$

Gaussian kernel to control coordination number
Penalty for atoms getting too close
Distance penalty

r_{ij} = Distance between qubit i and j

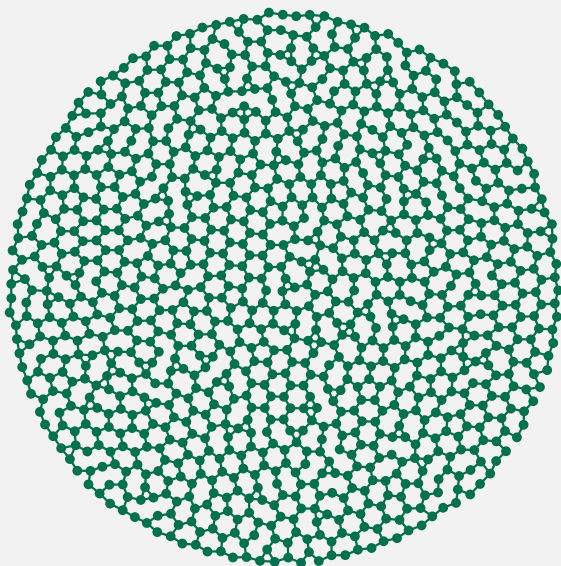
$k(r)$ = Gaussian function

m_j = Coordination numbers picked from normal distribution

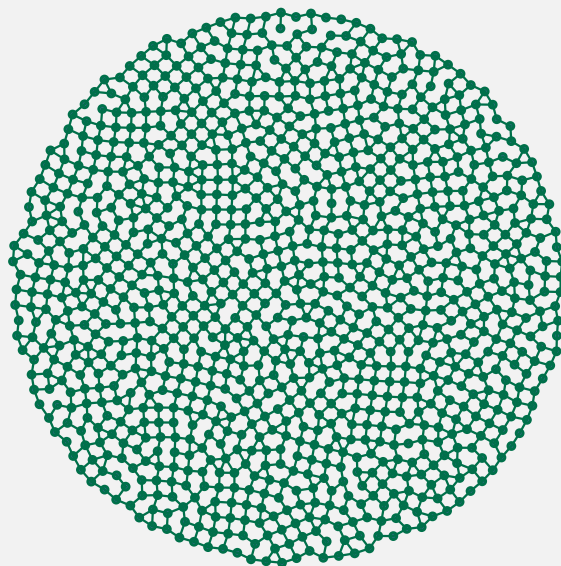
$a_1, a_2, \beta, \gamma, r_{\min}, r_{\max}$ = Hyper parameters

Examples of amorphous solids

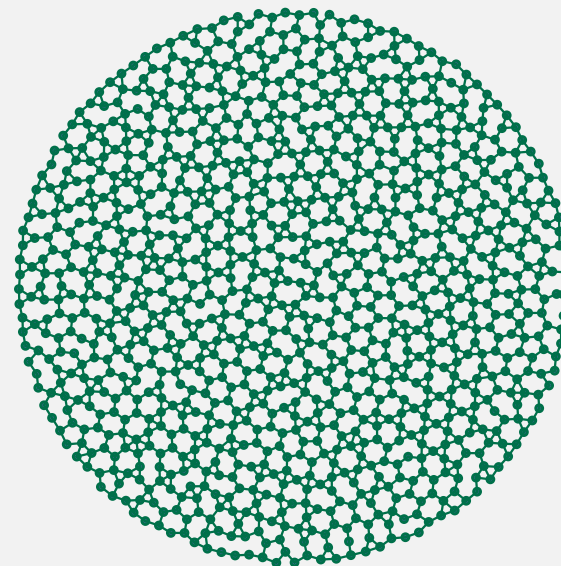
$C = 3$



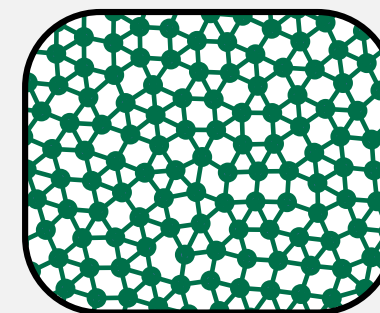
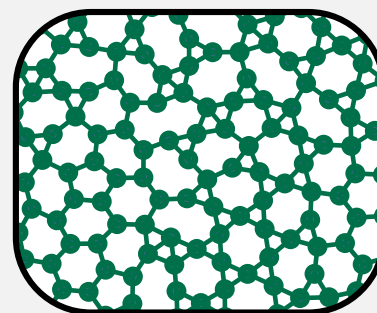
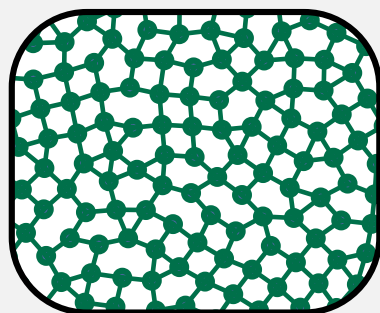
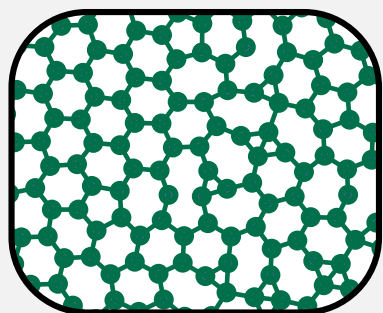
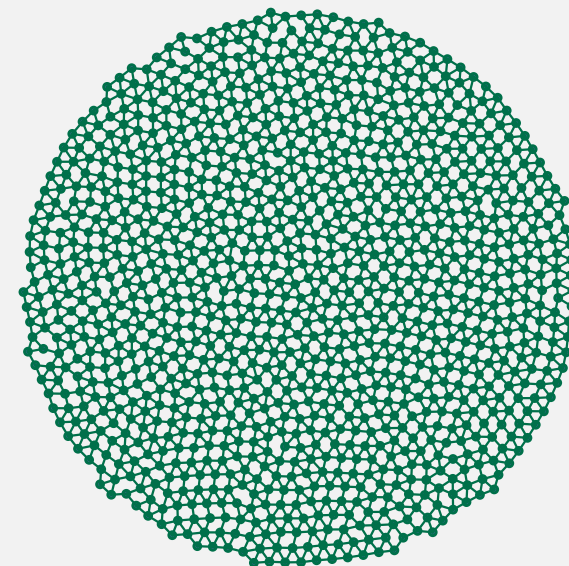
$C = 4$



$C = 3.5$



$C = 5$



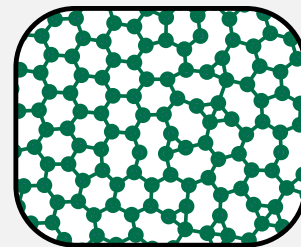
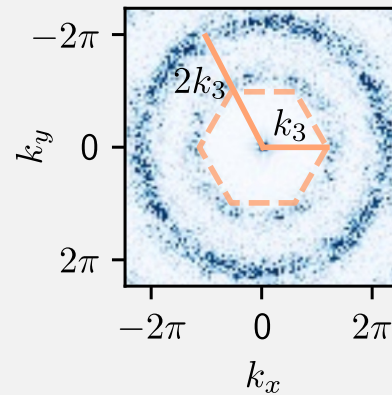
Static structure factor

Static structure factor

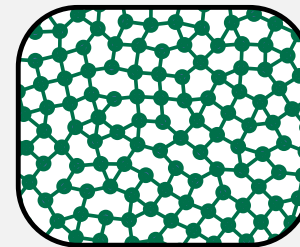
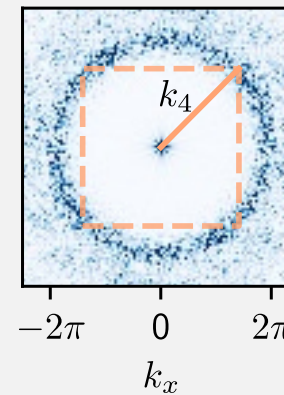
$$S(\mathbf{q}) = \frac{1}{N} \left| \sum_{j=1}^N e^{-\mathbf{q} \cdot \mathbf{R}_j} \right|^2$$

- No preferred direction
→ Rotational symmetry
- Same wave vector as dominant lattice (square, hexagonal)

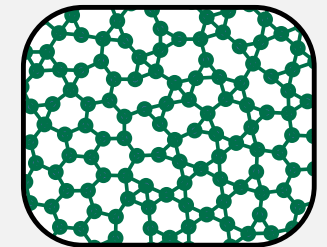
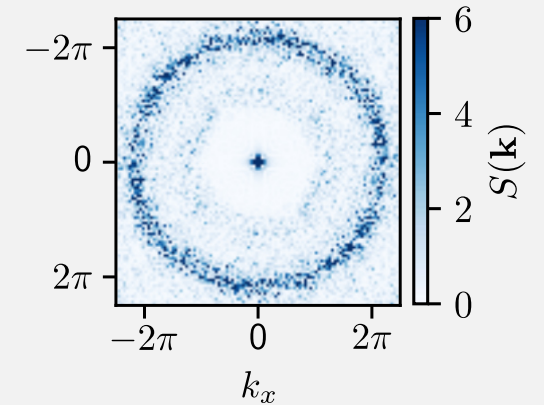
$C = 3$



$C = 4$

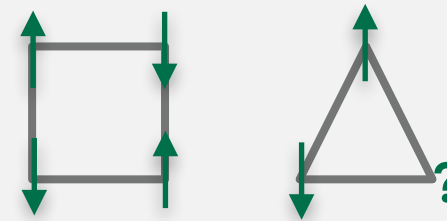
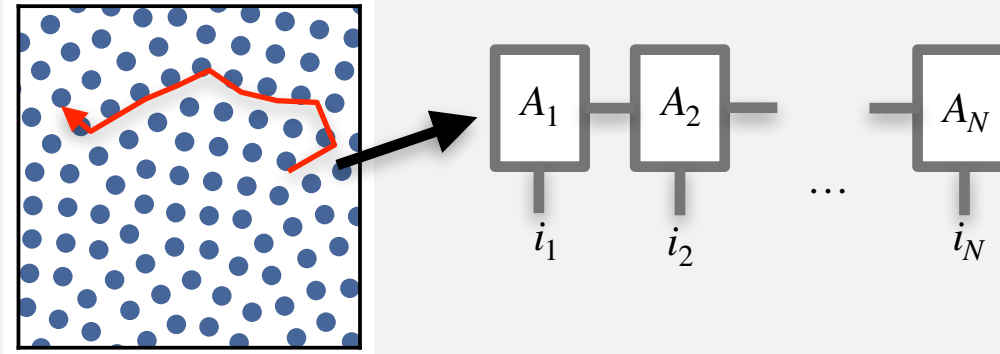


$C = 3.5$



Classical emulation of amorphous magnets

- Lack of lattice topology
→ challenge for the tensor network representation.
- Inherently requires large system sizes (due to boundary effects)
- In the antiferromagnetic case, presence of (local) frustration. How will this behave beyond regular lattices.



Semiclassical analysis

PROBLEM SET UP

- We consider the **ferromagnetic** Ising model with (allows us to avoid any frustration)

$$H = - \sum_{i<j} \frac{J_0}{r_{ij}^6} S_i^z S_j^z + h_x \sum_i S_i^x, \quad S_j^\alpha = \frac{1}{2} \sigma_j^\alpha.$$

- We set the minimum distance between two atoms to unity, such that: $\min r_{ij} = 1$
- We consider the transverse field h_x/\bar{J} , in which \bar{J} is the average nearest neighbour interaction strength
- We use mean-theory and linear spin wave theory to capture the physics of amorphous materials in the **semi-classical limit**

MEAN-FIELD PHASE DIAGRAM

Rotation to the mean-field polarised axis

$$S_i^z = \tilde{S}_i^z \cos \theta_i + \tilde{S}_i^x \sin \theta_i$$

$$S_i^x = \tilde{S}_i^x \cos \theta_i + \tilde{S}_i^z \sin \theta_i$$

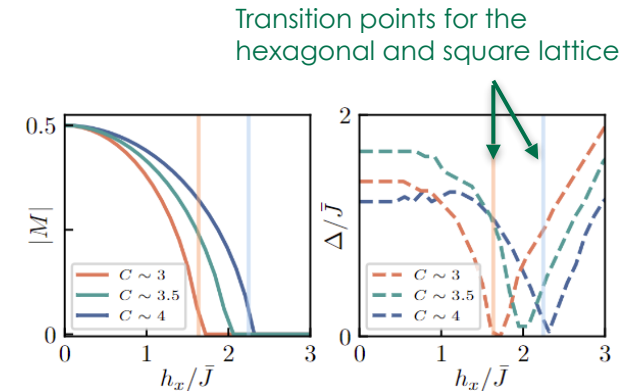
Δ : Linear spin wave theory energy gap

Under the assumption $\langle \tilde{S}_x \rangle \simeq 0$

$$E_{MF} = -\frac{1}{4} \sum_{i<j} \frac{J_0}{r_{ij}^6} \cos \theta_i \cos \theta_j - \frac{h_x}{2} \sum_i \sin \theta_i$$

Mean-field ferromagnetic order parameter

$$M = \frac{1}{N} \sum_i \langle S_i^z \rangle$$



(VERY BRIEF) REVIEW OF LINEAR SPIN WAVE THEORY

Holstein-Primakoff mapping

$$\tilde{S}_j^z = \frac{1}{2} - a_j^\dagger a_j, \quad \tilde{S}_j^x = \frac{1}{2} (a_j^\dagger + a_j)$$

$$\Rightarrow H = -\frac{1}{4} \sum_{i<j} \frac{J_0}{r_{ij}^6} \sin \theta_i \sin \theta_j (a_i^\dagger + a_i)(a_j^\dagger + a_j) + \sum_i \left[h_x \sin \theta_i + \frac{\cos \theta_i}{2} \sum_j \frac{J_0}{r_{ij}^6 \cos \theta_j} \right] a_i^\dagger a_i$$

Bogoliubov transformation

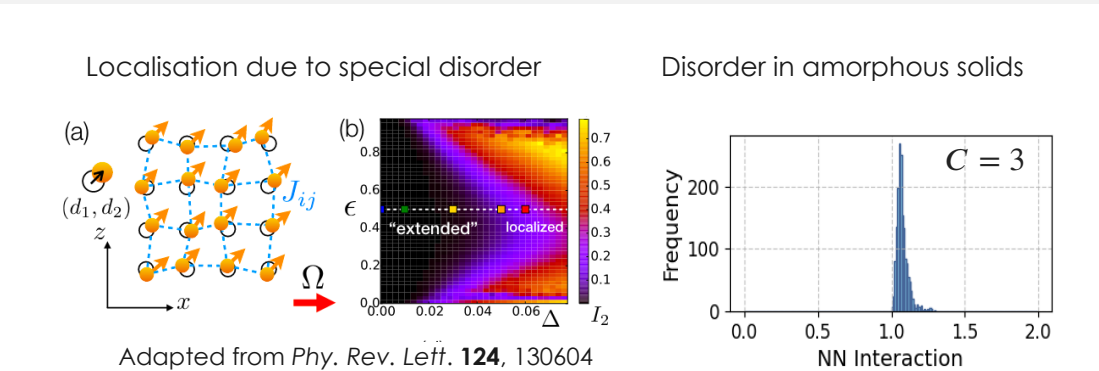
$$\Rightarrow H = \sum_{\mu=1}^N \omega_\mu b_\mu^\dagger b_\mu + E_g,$$

ω_μ : LSWT spectrum
 b_μ : LSWT eigenmodes

Semiclassical analysis

Linear spin wave theory

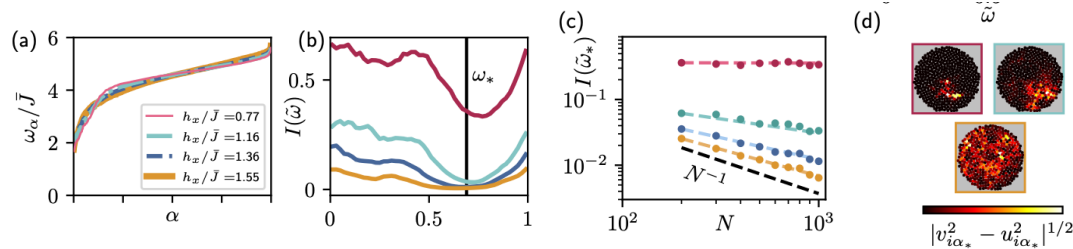
NATURE OF THE ENERGY SPECTRUM



We calculate **the inverse participation ratio**

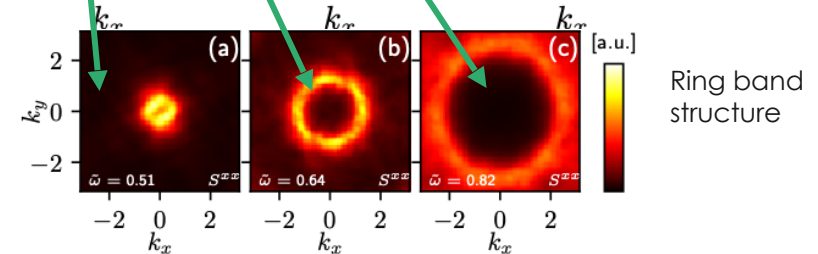
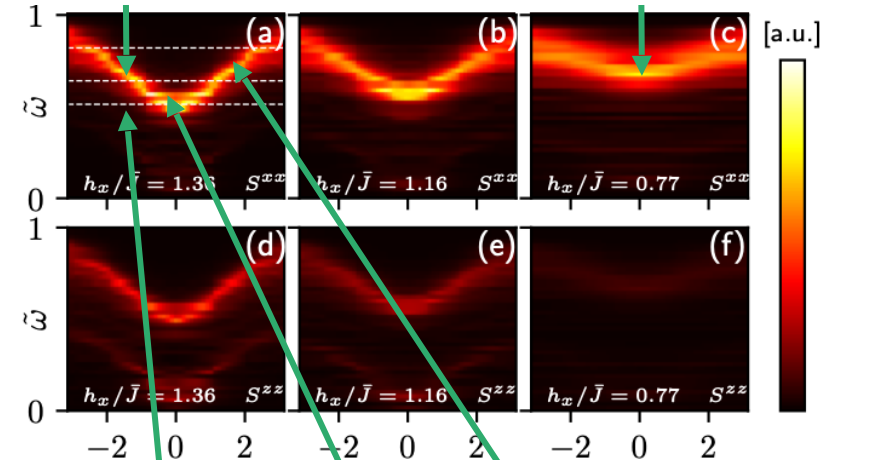
$$I(\omega) = \int_{r,w} |\Psi(\omega', r)|^4 \delta(\omega - \omega') dr$$

$I(\omega) \rightarrow 0$ for **delocalised** modes at energy ω



DYNAMICAL STRUCTURE FACTOR

Delocalized band despite apparent disorder Localisation (large momentum width) for small transverse field

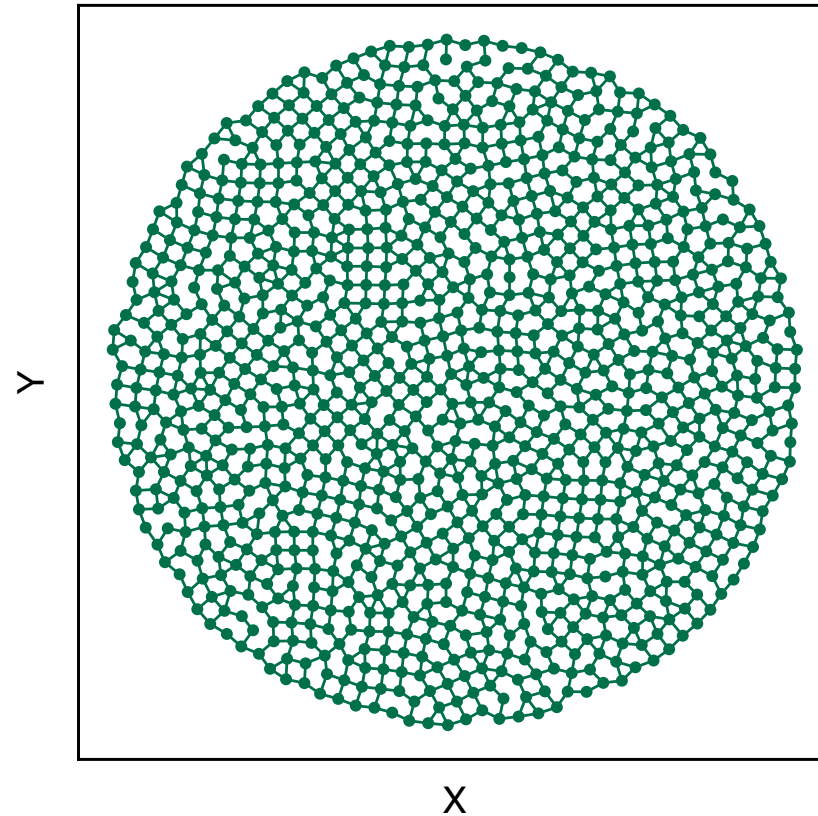


$$S^{\mu\nu}(k, \omega) \equiv \frac{1}{L} \sum_{ij} e^{ik(i-j)} \int_{-\infty}^{\infty} e^{i\omega t} S^{\mu\nu}(i, j, t) dt S^{\mu\nu}(i, j, t)$$

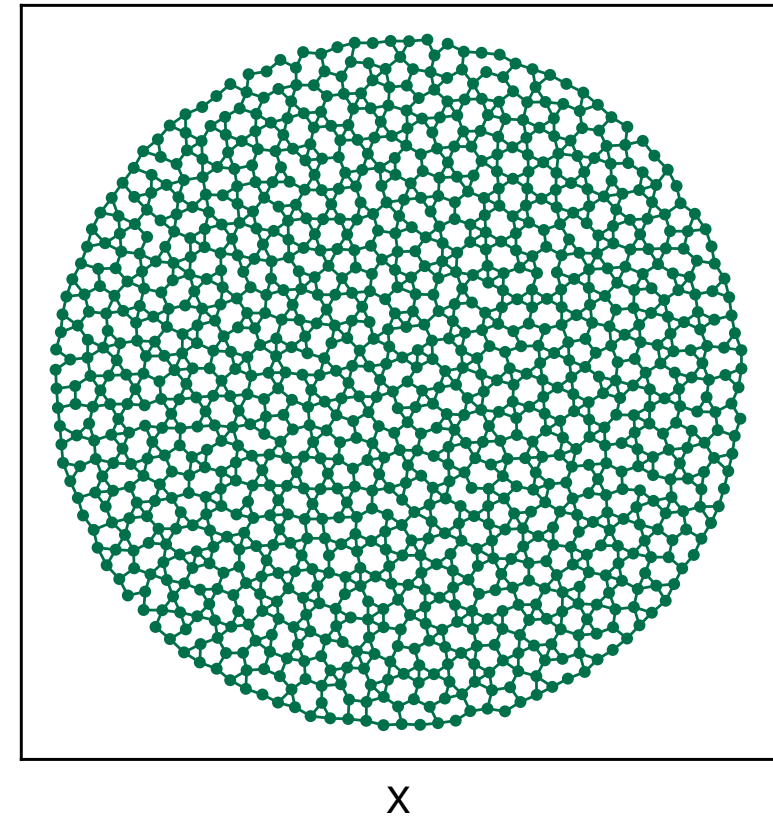
Geometrical frustration and disorder

- Both locally frustrated and unfrustrated plaquettes can coexist in an amorphous magnet
- For $C = 4$, we can generate amorphous magnets which bears similarities with square or Kagome lattices.
- This can lead to important differences already for classical spins:
 - regular square \rightarrow AF
 - kagome \rightarrow spin liquid

(a)



(b)



Classical simulated annealing

- We perform simulated annealing on $N = 60$ replicas.
- We then study statistical quantities such as
 - The energy of a replica

$$E_{SA}^\alpha = \langle H \rangle_\alpha$$

- The Edward-Anderson parameter q_{SA}^2

$$q_{SA}^{\alpha\beta} = \frac{1}{N} \sum_{i=1}^N \sigma_i^\alpha \sigma_i^\beta$$

$$q_{SA}^2 = \frac{1}{N_R(N_R - 1)} \sum_{\alpha \neq \beta} |q_{SA}^{\alpha\beta}|^2$$

- We also compute the probability distribution of the replica overlap $P(q_{SA}^{\alpha\beta})$ for 20 replicas with lowest energy.

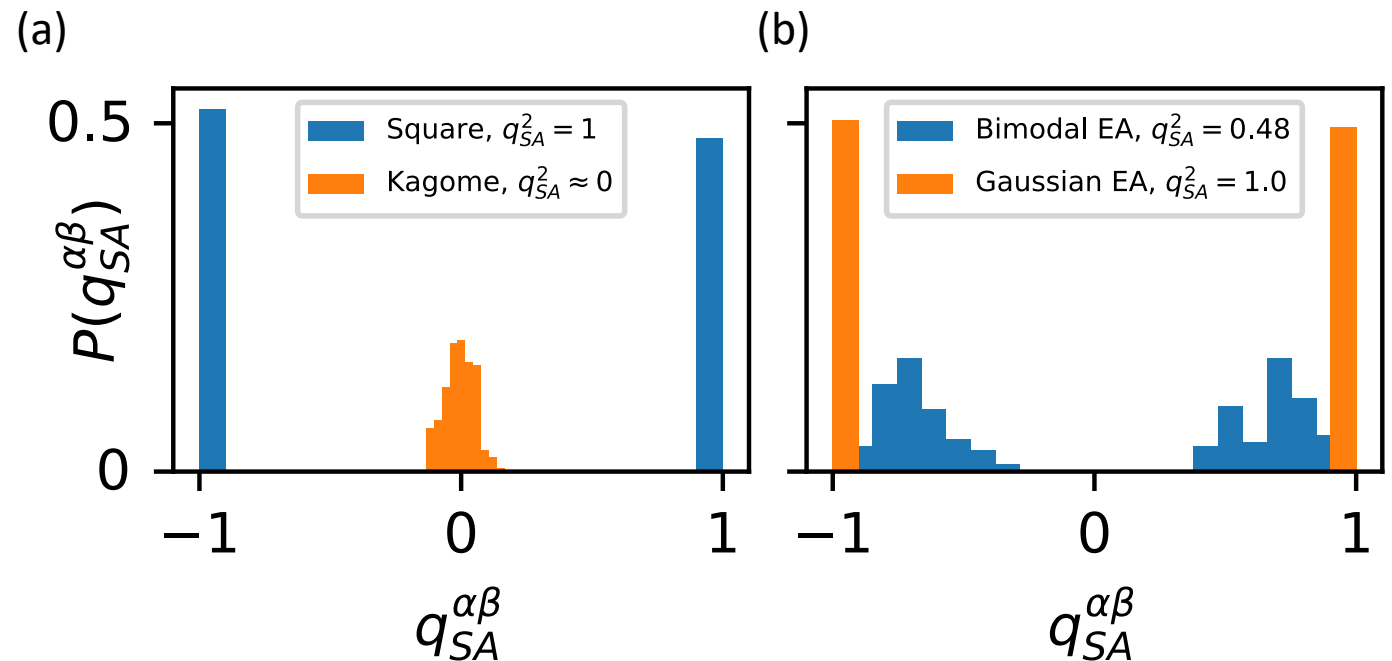
MONTE CARLO SWEEP

- random single spin flip
- Metropolis update with temperature T_i

$$T_i = T_0(1 - i/n_{\text{steps}}), i = 1, \dots, n_{\text{steps}}$$

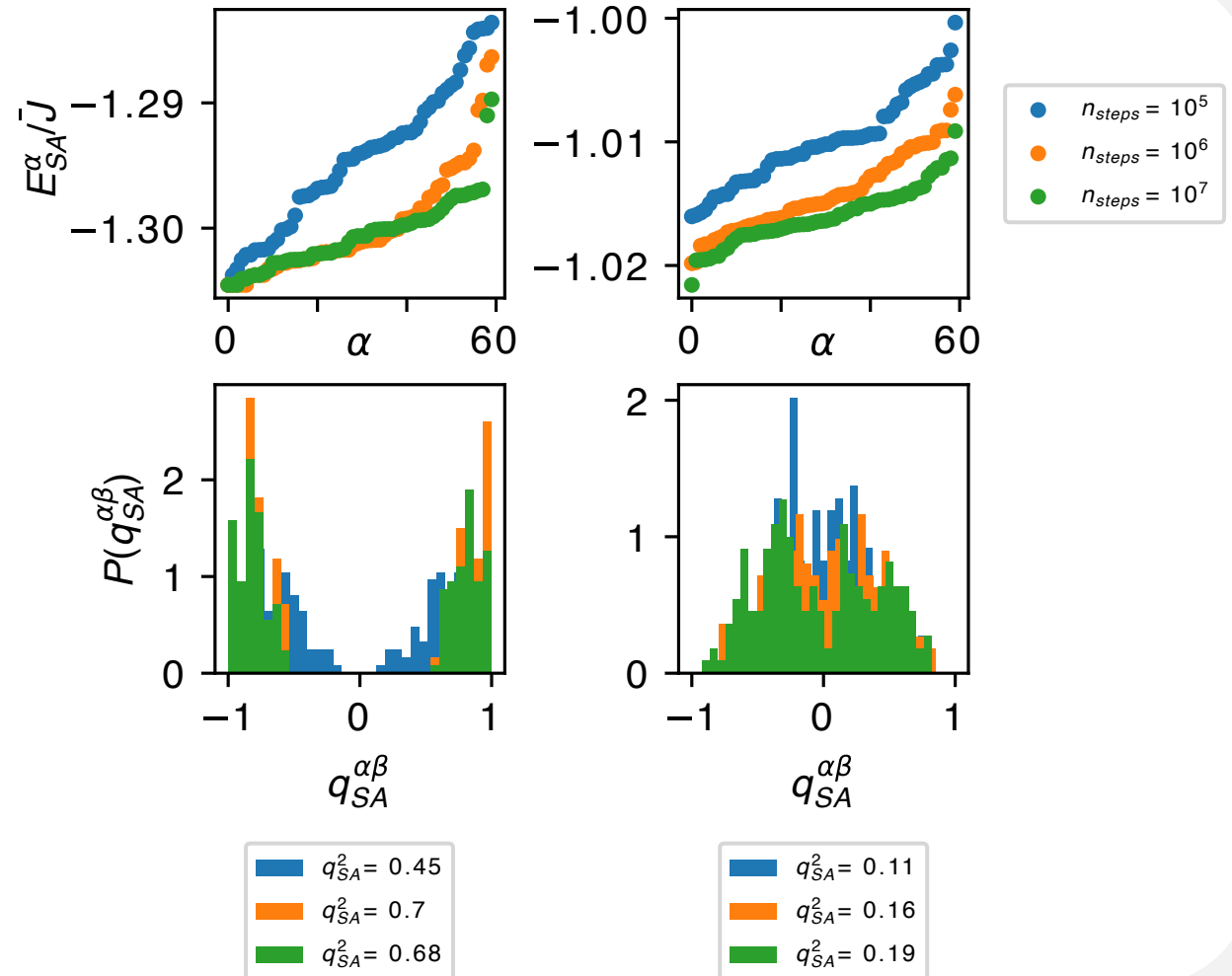
SA on paradigmatic models

- Different behaviour of the Probability distribution of the replica overlap for square and kagome (a).
- This reflects the difference between the AF GS and the spin liquid GS.
- We also show the differences between two paradigmatic examples of spin glasses: The Edward Anderson model with Bimodal couplings and Gaussian couplings (b).
- Important to note that SA converged well for the spin glass because of the small system sizes considered here (6x6)



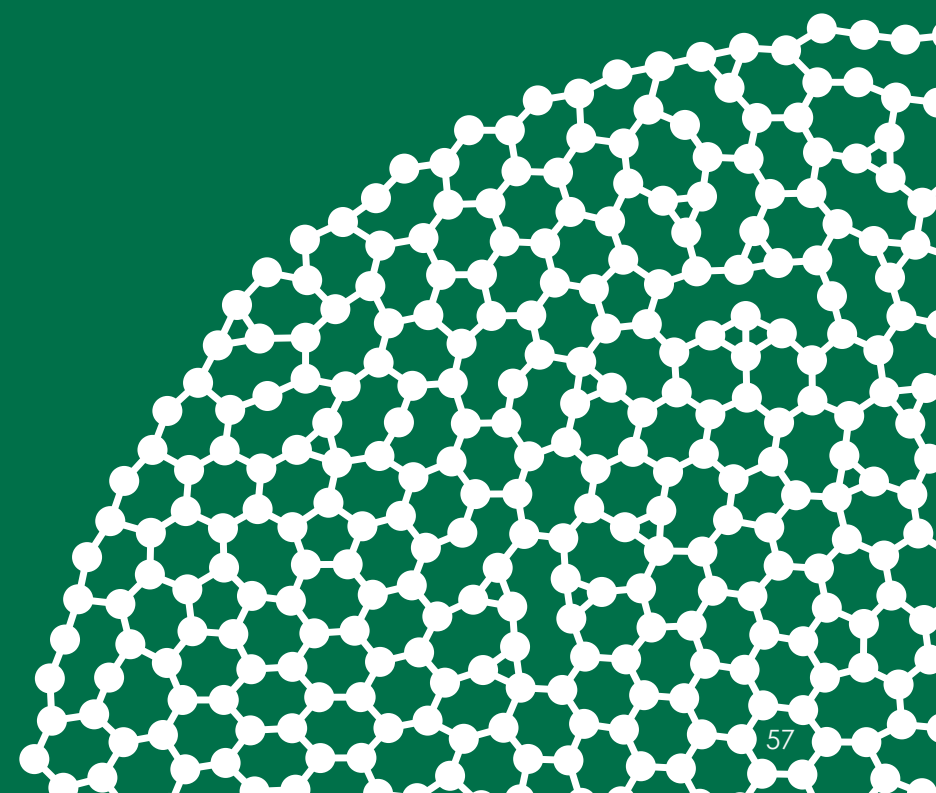
SA on amorphous materials

- We perform a similar study for the amorphous solid with $C \approx 4$ for both square and kagome types and for $N = 400$.
- SA does not converge well in this case (see (a,b)). This features also happens for spin glasses of the EA type.
- Strong difference between the energy landscape of square and kagome amorphous solids.
- Beware that we explore the low energy landscape but not the GS due to the lack of convergence.

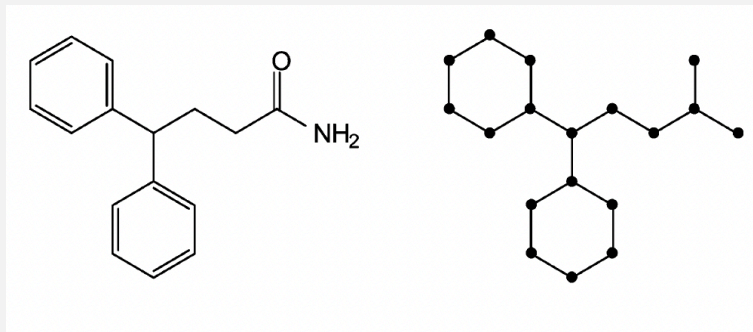


4

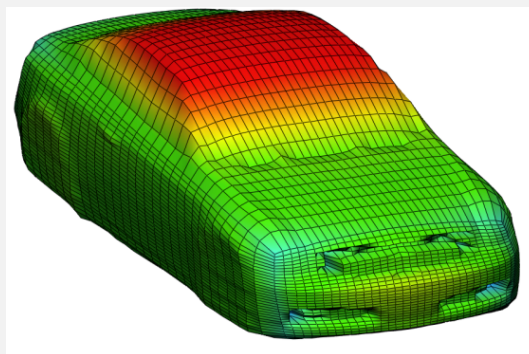
Quantum evolution kernel



Graph-structured data



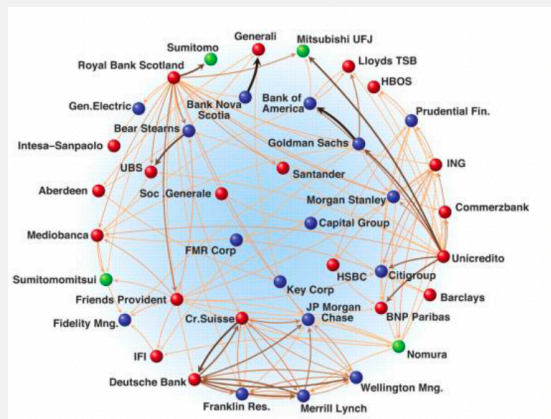
Molecules



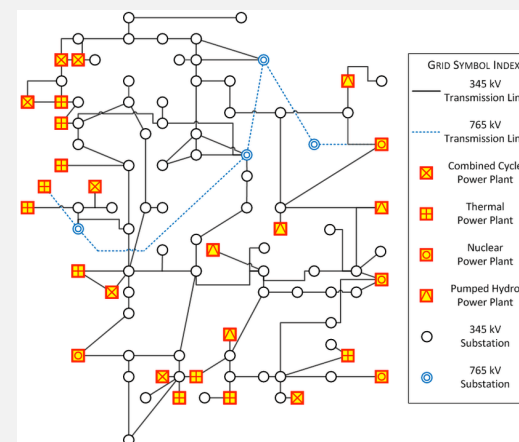
3D shapes



Social networks



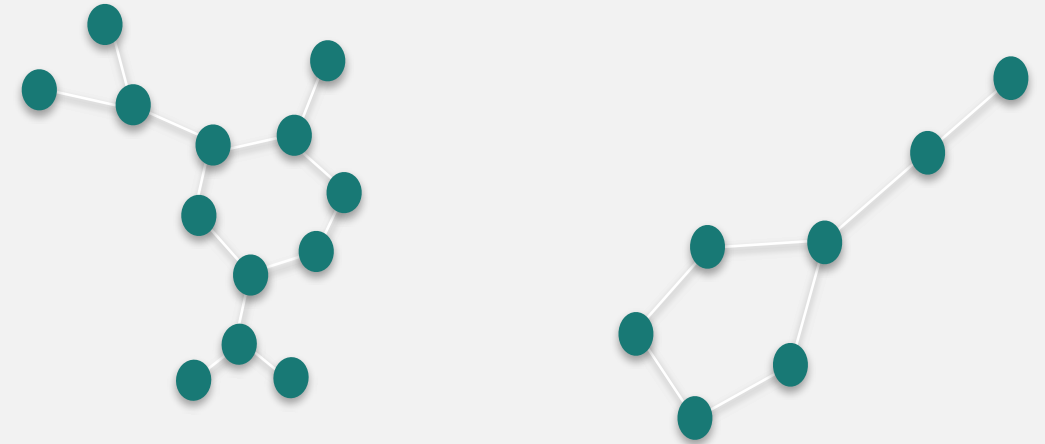
Economic networks





Power networks

Toxicity screening on Iroise

Predictive Toxicity Challenge on Female Mice [1,2]



- First graph QML implementation on a real dataset of such size.
- Year-long internal R&D project involving sw and hw teams

# of registers # of qubits	 Control	 Runtime
288 registers, up to 32 qubits	Global analog, constant pulses	~120k shots

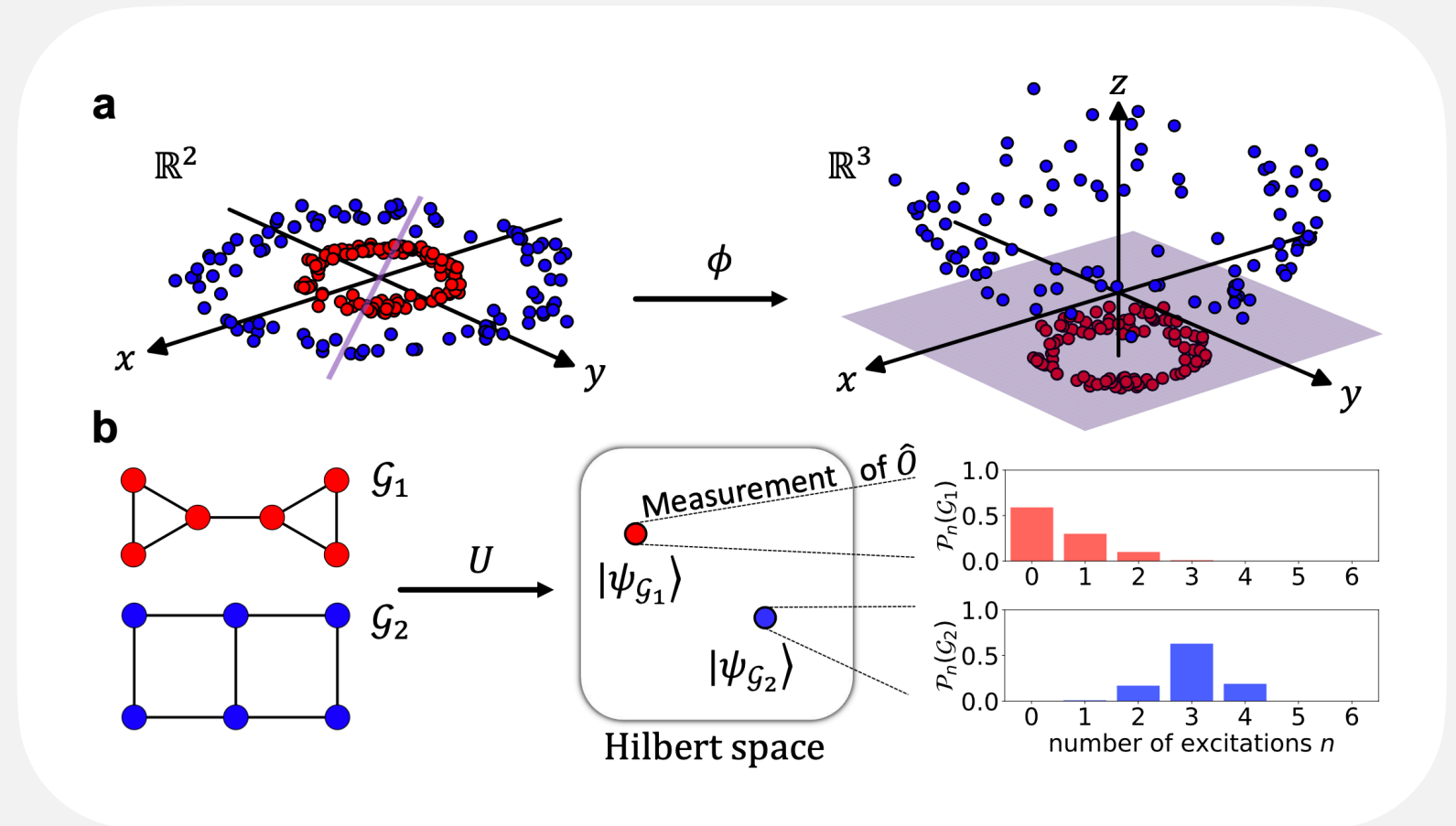
- Albrecht B, Dalyac C et al. "Quantum feature maps for graph machine learning on a neutral atom quantum processor." *Physical Review A* 107.4 (2023): 042615.

[1] Helma, et al., *Bioinformatics*, 01, 1, 107-108 (2001)

[2] Data taken from the GraKeL library

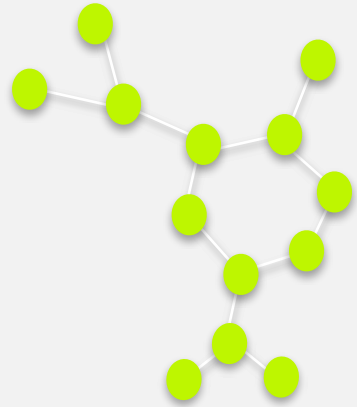
Using the quantum dynamics to embed the data

- The quantum dynamics is expected to introduce a richer feature map, with characteristics that are hard to access by classical means



Quantum feature map

The graph topology is encoded in the dynamics through the Hamiltonian of the system



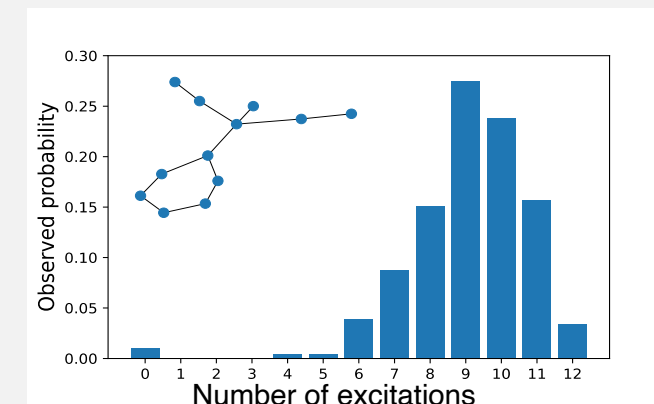
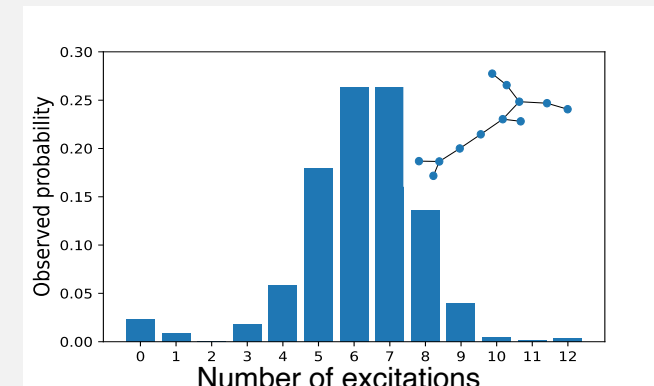
Creates an edge if
 $r_{ij} < r_0$

$$G = \{V, E\}$$



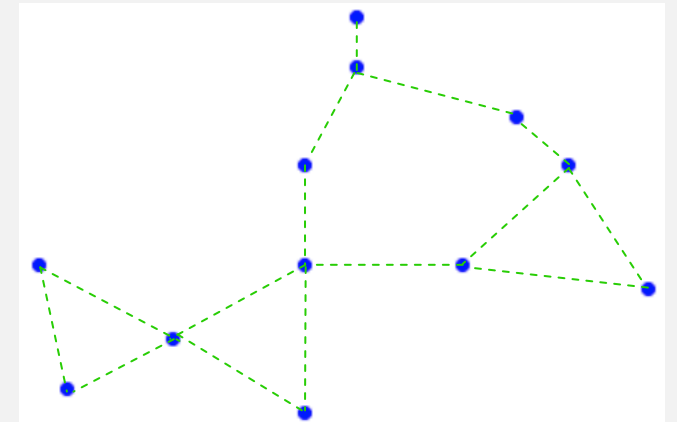
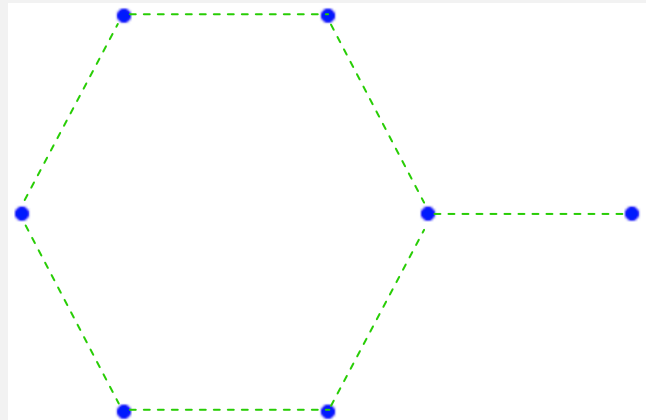
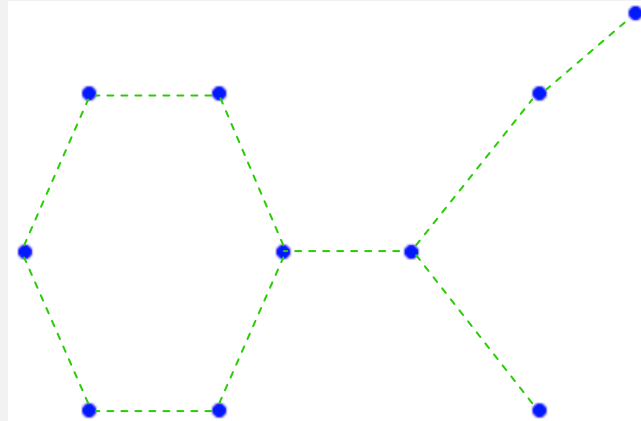
$$H_G \sim \sum_{i,j} V_{ij} n_i n_j$$

The measurement histograms enable us to build a similarity measure between graphs

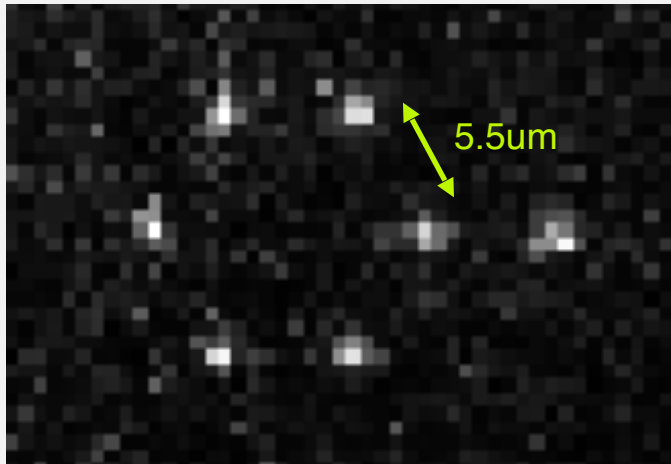
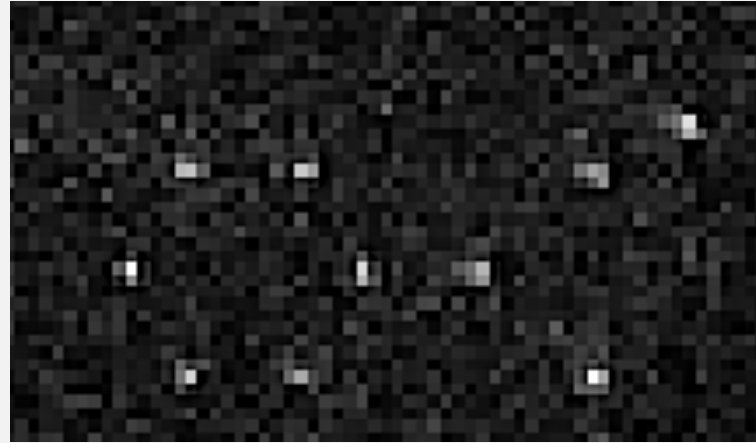


Jensen-Shannon divergence between the graphs

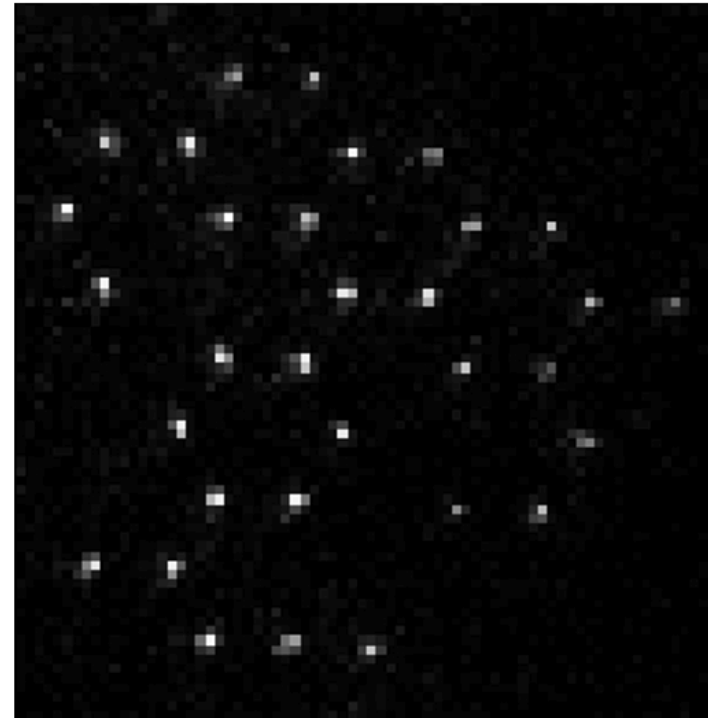
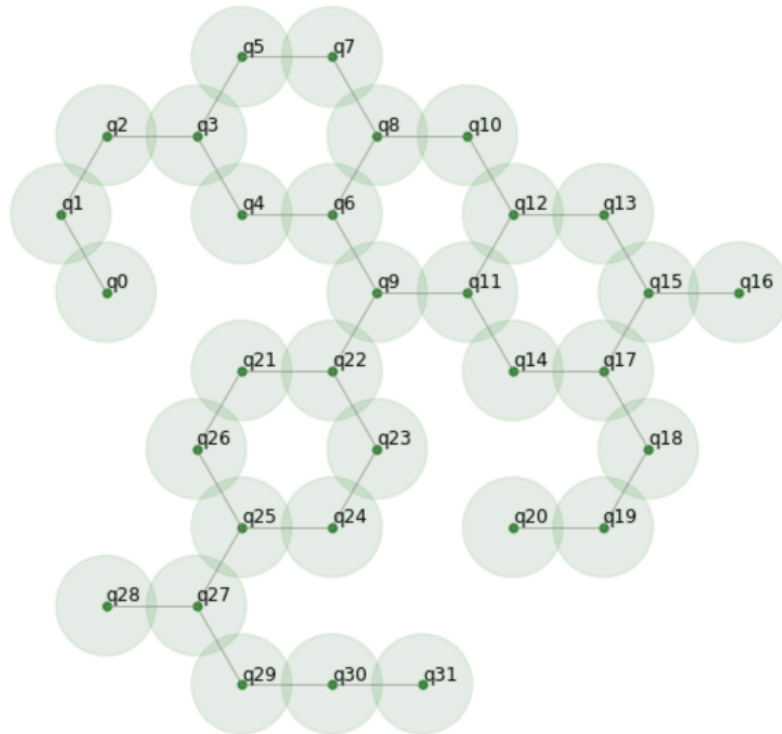
Chemical compounds in PTC-FM



Chemical compounds in PTC-FM



Large atom number registers



Experimental results on par with **classical kernel**

Classification results on par with the best classical kernels on this dataset

Kernel	F_1 -score (%)
QEK	60.4 ± 5.1
SVM- ϑ	58.2 ± 5.5
Graphlet Sampling	56.9 ± 5.0
Random Walk	55.1 ± 6.9
Shortest Path	49.8 ± 6.0

